Appendix A.36:

Randolph St – CPT 44440

Table 1: Site Description for Randolph St (CPT 44440).

Attribute	Yes/No			Description/Date	Symbol in Figure 1
	10-m Buffer	20-m Buffer	50-m Buffer		
Near a body of surface water or other free face features?	No	No	No	The center of the site is ~60 m to the NE from the unnamed stream/channel (~0.5-1-m high free-face feature) and ~380 m to the SW from the unnamed canal (~1-m high free-face feature).	NA
Lateral spreading observed during the CES?	No	No	No	No lateral spreading was observed by the mapping team.[1]	NA
Nearby buildings or structures?	Yes	Yes	Yes	Building coverage of the 10-, 20-, and 50-m buffers is 16, 23, and 20%, respectively. Buildings are in the NW and SW quadrants of the 10-m buffer, NE, NW, and SW quadrants of the 20-m buffer, and all quadrants of the 50-m buffer.	White Fill + Brown Outline
Sloping land?	No	No	No	Flat land, residential area	NA
Step changes in the ground surface?	No	No	No	NA	NA
Retaining walls?	No	No	No	NA	NA
Vegetation?	Yes	Yes	Yes	Trees and bushes cover 3, 6, and 15% of the 10-, 20-, and 50-m buffers, respectively. They are in the NE, NW, and SW quadrants of the 10- and 20-m buffers and all quadrants of the 50-m buffer.	White Fill + Green Outline
Anthropogenic changes to the site between the LiDAR surveys?	Yes	Yes	Yes	Road construction in 2007 most likely affected the 10- and 20-m buffers in addition to the 50-m buffer. Vegetation, building removal, and building addition in the SW quadrant of the 50-m buffer between Feb 2006 and Mar 2009. Road construction in Sep 2010 and between Mar 2013 and Aug 2013, affected all buffers. Building removal in the E portion of the 50-m buffer between Aug 2013 and Jan 2013. Building removal in the E portion of the 50-m buffer between Aug 2014 and Sep 2014. Building addition at the latter property between Jan 2015 and July 2015. Removal of structures in the SW quadrant of the 50-m buffer between July 2015 and Sep 2015.	Building Addition/ Removal: Orange Crossline; Vegetation Removal: Green Outline
Other important factors?	Yes	Yes	Yes	Low-motor-vehicle-volume, two-way road (Randolph St) occupies 10, 23, and 20% of the 10-, 20-, and 50-m buffers, respectively, and runs in the NE-SW direction through the NE, SE, and SW quadrants.	Road: Gray Fill + Red Outline

Note: Buffer is the area within a circle of a specified radius with CPT investigations done at its center (172.669546°, -43.539782°).

[1] Canterbury Geotechnical Database. (2012). "Observed Ground Crack Locations", Map Layer CGD0400 - 23 July 2012, retrieved July 09, 2018 from https://canterburygeotechnicaldatabase.projectorbit.com/

Figure 1: Site plan with areas where ejecta-induced settlement is considered.

Note 1: Two patches (outlined in red) in the free field were selected for the settlement assessment as areas free of vegetation and structures. Other important factors considered in the selection process were the proximity of a patch to a CPT, a property subjected to addition and/or demolition of a structure, and front yard/backyard alterations (e.g., ploughing, rubble, scrap), and aerial distribution of sediment ejecta. In addition, the entire portion of the road within the 50-m buffer was considered for settlement assessment. Roads as hard, relatively flat surfaces provide many ground-classified points. The Sep-10 and Dec-11 LiDAR-based settlement analyses were not conducted due to the evident absence of ejecta from Patches A and B and Road. The LiDAR-based settlement analyses of the Road were not performed for the Feb-11 EQ due to the anthropogenic changes that had the potential to affect the Sep 2010 LiDAR survey.

Table 2: LiDAR flight error adjustments, global adjustments for the difference between average LiDAR point elevations and benchmark survey elevations, and vertical tectonic movement adjustments.

	Adjustments (mm)		
Earthquake Event(s)	LiDAR Flight Error	Global Offset[2]	Tectonic Vertical Movement
Sep-10	-100	-3	0
Feb-11	+100	16	+30
Jun-11	0	38	-45
Dec-11	-50	-65	+15
CES	-50	-14	0
Any LiDAR survey affected by ejecta?			No

Note: The negative sign indicates the subtraction from the ground surface subsidence, while the positive sign indicates the addition to the ground surface subsidence.

Table 3a: LiDAR Measurement Error for Patch A.

Surveys	Buffer	Area Averaged Difference Indicating Repeat Measurement Error (mm)	$\sigma^*_{\text{individual LiDAR points}}$ (mm)	%Reduction in σ due to Area Averaging of LiDAR Points
Post Feb 2011: Mar 2011 and May 2011	10-m	74	59	[125,125]
	20-m	74		
	50-m	74		
Post Dec 2011: Feb 2012 and Oct 2015	10-m	ND	70	[ND,ND]
	20-m	ND		
	50-m	ND		

*Standard deviation; ND = Not determined.

[2] Russell, J., & van Ballegooy, S. (2015). *Canterbury Earthquake Sequence: Increased liquefaction vulnerability assessment methodology*. New Zealand: Tonkin & Taylor Ltd.

Table 3b: LiDAR Measurement Error for Patch B.

Surveys	Buffer	Area Averaged Difference Indicating Repeat Measurement Error (mm)	$\sigma^*_{\text{individual LiDAR points}}$ (mm)	%Reduction in σ due to Area Averaging of LiDAR Points
Post Feb 2011: Mar 2011 and May 2011	10-m	NA	59	[90,90]
	20-m	ND		
	50-m	53		
Post Dec 2011: Feb 2012 and Oct 2015	10-m	ND	70	[ND,ND]
	20-m	ND		
	50-m	ND		

*Standard deviation; NA = Not available; ND = Not determined.

Table 3c: LiDAR Measurement Error for Road.

Surveys	Buffer	Area Averaged Difference Indicating Repeat Measurement Error (mm)	$\sigma^*_{\text{individual LiDAR points}}$ (mm)	%Reduction in σ due to Area Averaging of LiDAR Points
Post Feb 2011: Mar 2011 and May 2011	10-m	39	59	[2,51]
	20-m	30		
	50-m	1		
Post Dec 2011: Feb 2012 and Oct 2015	10-m	ND	70	[ND,ND]
	20-m	ND		
	50-m	ND		

*Standard deviation; ND = Not determined.

Table 4a: Ground surface subsidence adjustments due to LiDAR measurement error for Patch A.

Earthquake Event(s)	$\sigma_{\text{pre-EQ LiDAR survey}}$ (mm)	$\sigma_{\text{post-EQ LiDAR survey}}$ (mm)	σ_{total} (mm)	Area Average Adjusted σ (mm) **
Sep-10	158	56	134	±168
Feb-11	56	59	59	±74
Jun-11	59	61	62	±78
Dec-11	61	70	87	±109
CES	158	70	124	±156

**Based on the highest %Reduction in Table 3a.

Table 4b: Ground surface subsidence adjustments due to LiDAR measurement error for Patch B.

Earthquake Event(s)	$\sigma_{\text{pre-EQ LiDAR survey}}$ (mm)	$\sigma_{\text{post-EQ LiDAR survey}}$ (mm)	σ_{total} (mm)	Area Average Adjusted σ (mm) **
Sep-10	158	56	134	±120
Feb-11	56	59	59	±53
Jun-11	59	61	62	±56
Dec-11	61	70	87	±78
CES	158	70	124	±112

**Based on the highest %Reduction in Table 3b.

Table 4c: Ground surface subsidence adjustments due to LiDAR measurement error for Road.

Earthquake Event(s)	$\sigma_{\text{pre-EQ LiDAR survey}}$ (mm)	$\sigma_{\text{post-EQ LiDAR survey}}$ (mm)	σ_{total} (mm)	Area Average Adjusted σ (mm) **
Sep-10	158	56	134	±68
Feb-11	56	59	59	±30
Jun-11	59	61	62	±32
Dec-11	61	70	87	±44
CES	158	70	124	±63

**Based on the highest %Reduction in Table 3c.

Table 5a: Raw liquefaction-related ground surface subsidence using original LiDAR points for Patch A.

	Average Ground Surface Subsidence (mm)		
Earthquake Event(s)	10-m Buffer	20-m Buffer	50-m Buffer
Sep-10	ND	ND	ND
Feb-11	-116	-116	-116
Jun-11	58	58	58
Dec-11	ND	ND	ND
CES	ND	ND	ND

Table 5b: Raw liquefaction-related ground surface subsidence using original LiDAR points for Patch B.

	Average Ground Surface Subsidence (mm)		
Earthquake Event(s)	10-m Buffer	20-m Buffer	50-m Buffer
Sep-10	NA	ND	ND
Feb-11	NA	ND	-59
Jun-11	NA	ND	43
Dec-11	NA	ND	ND
CES	NA	ND	ND

Table 5c: Raw liquefaction-related ground surface subsidence using original LiDAR points for Road.

	Average Ground Surface Subsidence (mm)		
Earthquake Event(s)	10-m Buffer	20-m Buffer	50-m Buffer
Sep-10	ND	ND	ND
Feb-11	ND	ND	ND
Jun-11	54	50	38
Dec-11	ND	ND	ND
CES	ND	ND	ND

Table 6a: Corrected liquefaction-related ground surface subsidence using original LiDAR points for Patch A with the calculated adjustments in Table 2.

	Average Calculated Ground Surface Subsidence (mm)		
Earthquake Event(s)	10-m Buffer	20-m Buffer	50-m Buffer
Sep-10	ND	ND	ND
Feb-11	30±75	30±75	30±75
Jun-11	51±75	51±75	51±75
Dec-11	ND	ND	ND
CES	ND	ND	ND

Notes: Plus/minus values are same as those in Table 4a, but rounded to the nearest 25 mm; Positive overall values indicate ground surface subsidence, while negative overall values indicate ground surface uplift; ND = not determined.

Table 6b: Corrected liquefaction-related ground surface subsidence using original LiDAR points for Patch B with the calculated adjustments in Table 2.

	Average Calculated Ground Surface Subsidence (mm)		
Earthquake Event(s)	10-m Buffer	20-m Buffer	50-m Buffer
Sep-10	NA	ND	ND
Feb-11	NA	ND	88±50
Jun-11	NA	ND	36±50
Dec-11	NA	ND	ND
CES	NA	ND	ND

Notes: Plus/minus values are same as those in Table 4b, but rounded to the nearest 25 mm; Positive overall values indicate ground surface subsidence, while negative overall values indicate ground surface uplift; NA = Not available; ND = Not determined.

Table 6c: Corrected liquefaction-related ground surface subsidence using original LiDAR points for Road with the calculated adjustments in Table 2.

	Average Calculated Ground Surface Subsidence (mm)		
Earthquake Event(s)	10-m Buffer	20-m Buffer	50-m Buffer
Sep-10	ND	ND	ND
Feb-11	ND	ND	ND
Jun-11	47±25	43±25	31±25
Dec-11	ND	ND	ND
CES	ND	ND	ND

Notes: Plus/minus values are same as those in Table 4c, but rounded to the nearest 25 mm; Positive overall values indicate ground surface subsidence, while negative overall values indicate ground surface uplift; ND = Not determined.

Table 7a: Corrected liquefaction-related ground surface subsidence for Patch A using LiDAR DEMs.

	Estimated Ground Surface Subsidence (mm)								
	10-m Buffer			20-m Buffer			50-m Buffer		
Earthquake Event(s)	16th %ile	50th %ile	84th %ile	16th %ile	50th %ile	84th %ile	16th %ile	50th %ile	84th %ile
Sep-10	<50	<50	<50	<50	<50	<50	<50	<50	<50
Feb-11	100	100	150	100	100	150	100	100	150
Jun-11	<50	50	50	<50	50	50	<50	50	50
Dec-11	50	50	100	50	50	100	50	50	100
CES	100	150	150	100	150	150	100	150	150

Note: These percentiles are not the exact statistical measures; they indicate the spatial variability of ground surface subsidence; NA = Not available; ND = Not determined.

Table 7b: Corrected liquefaction-related ground surface subsidence for Patch B using LiDAR DEMs.

	Estimated Ground Surface Subsidence (mm)								
	10-m Buffer			20-m Buffer			50-m Buffer		
Earthquake Event(s)	16th %ile	50th %ile	84th %ile	16th %ile	50th %ile	84th %ile	16th %ile	50th %ile	84th %ile
Sep-10	NA	NA	NA	ND	ND	ND	<50	<50	<50
Feb-11	NA	NA	NA	ND	ND	ND	100	100	150
Jun-11	NA	NA	NA	ND	ND	ND	<50	50	50
Dec-11	NA	NA	NA	ND	ND	ND	<50	<50	50
CES	NA	NA	NA	ND	ND	ND	100	200	250

Note: These percentiles are not the exact statistical measures; they indicate the spatial variability of ground surface subsidence; NA = Not available; ND = Not determined.

Table 7c: Corrected liquefaction-related ground surface subsidence for Road using LiDAR DEMs.

	Estimated Ground Surface Subsidence (mm)								
	10-m Buffer			20-m Buffer			50-m Buffer		
Earthquake Event(s)	16th %ile	50th %ile	84th %ile	16th %ile	50th %ile	84th %ile	16th %ile	50th %ile	84th %ile
Sep-10	ND	ND	ND	ND	ND	ND	ND	ND	ND
Feb-11	ND	ND	ND	ND	ND	ND	ND	ND	ND
Jun-11	<50	50	50	<50	50	50	<50	50	50
Dec-11	<50	<50	50	<50	<50	50	<50	<50	50
CES	ND	ND	ND	ND	ND	ND	ND	ND	ND

Note: These percentiles are not the exact statistical measures; they indicate the spatial variability of ground surface subsidence; ND = Not determined.

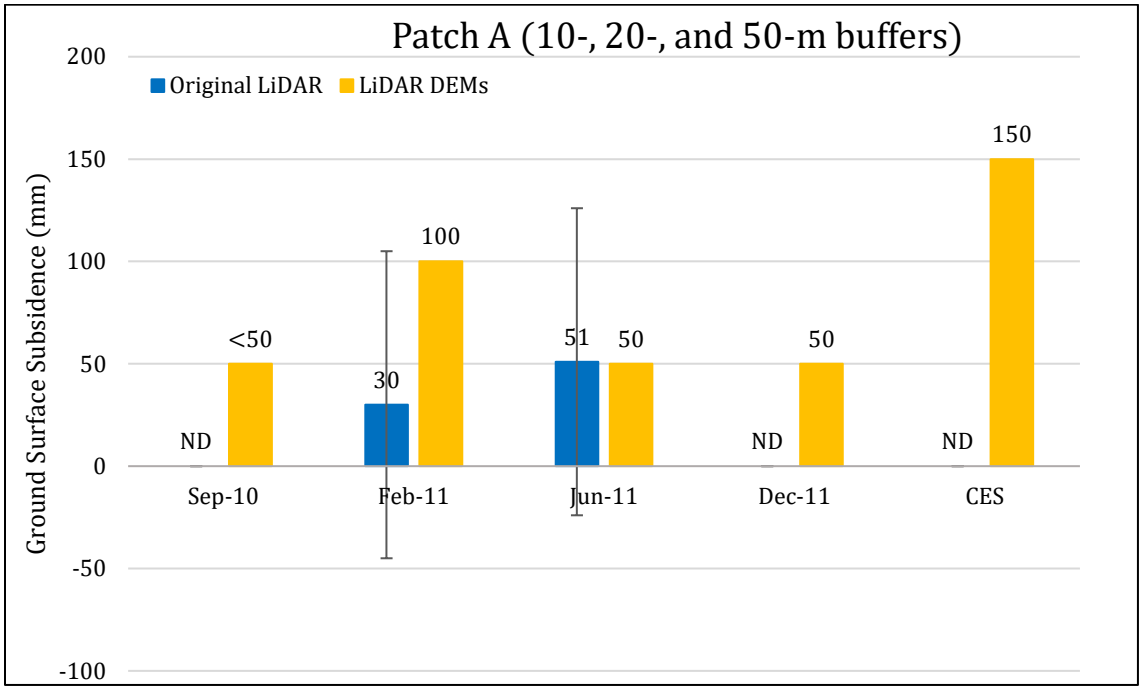

Figure 2: Comparison between ground surface subsidence determined from original LiDAR survey points and ground surface subsidence (50th %ile) estimated using LiDAR DEMs for Patch A (10-, 20-, and 50-m buffers).

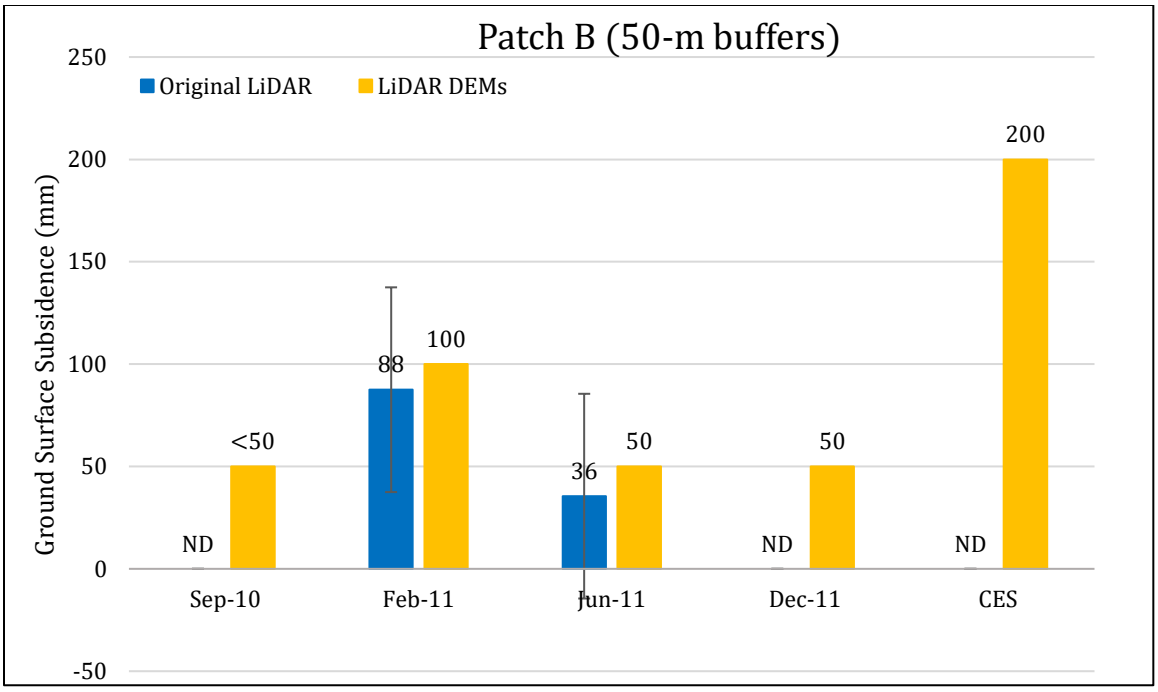

Figure 3: Comparison between ground surface subsidence determined from original LiDAR survey points and ground surface subsidence (50th %ile) estimated using LiDAR DEMs for Patch B (50-m buffer).

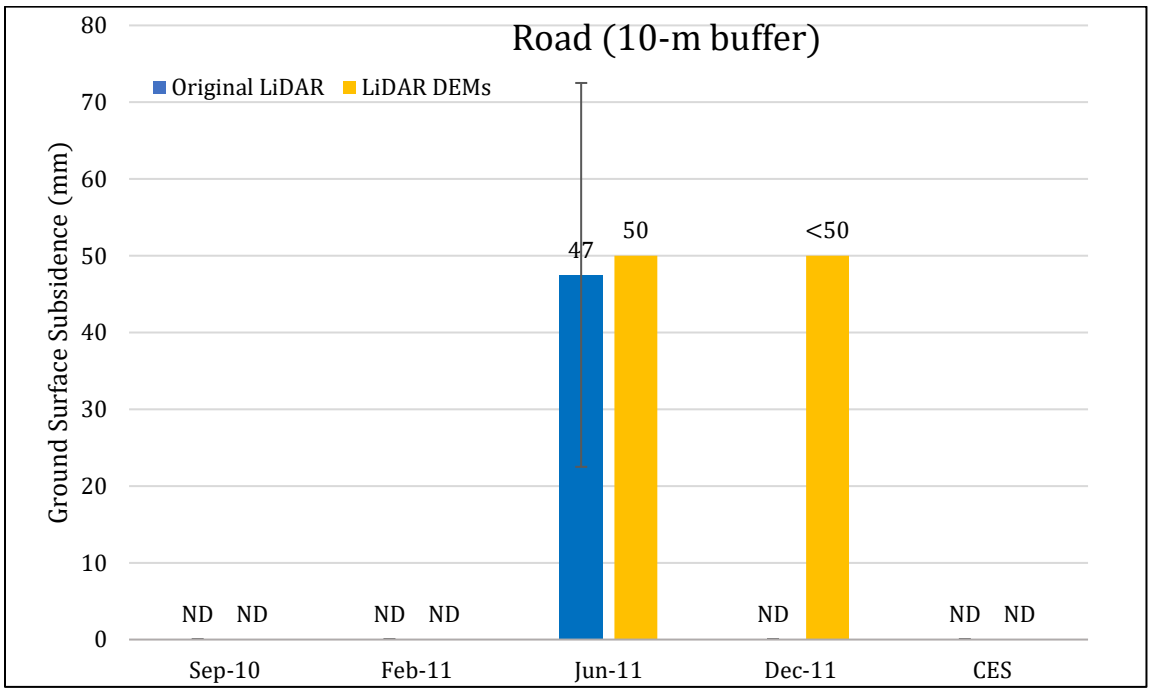

Figure 4: Comparison between ground surface subsidence determined from original LiDAR survey points and ground surface subsidence (50th %ile) estimated using LiDAR DEMs for Road (10-m buffer).

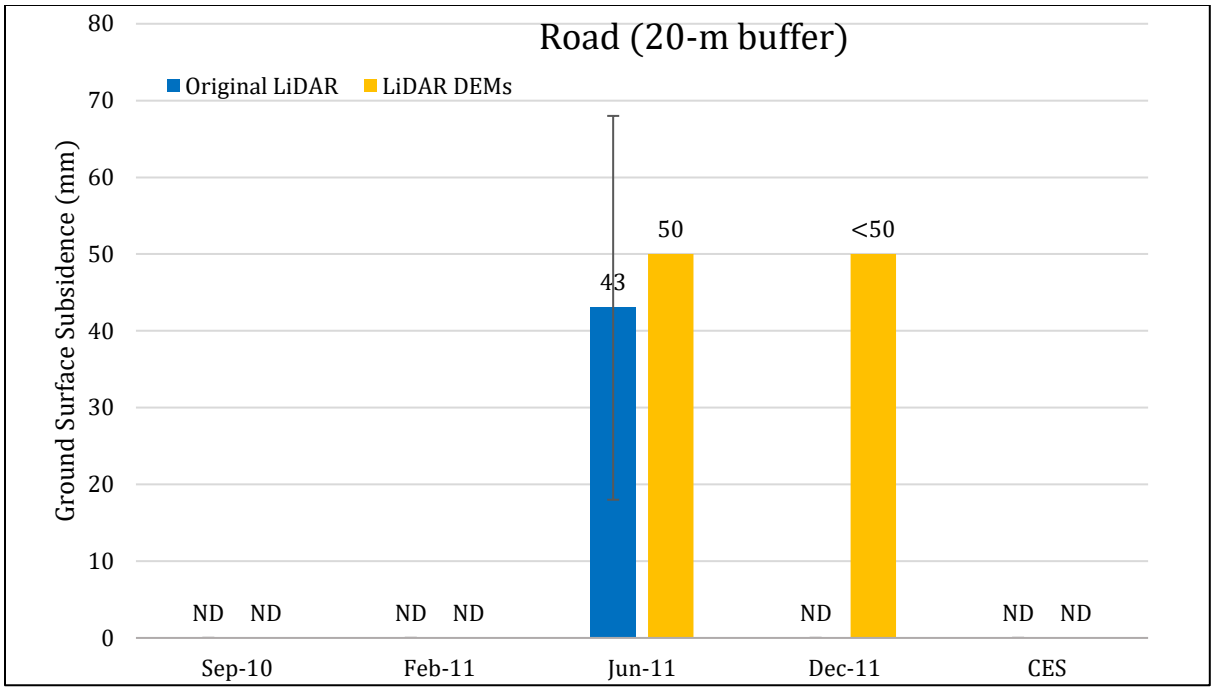

Figure 5: Comparison between ground surface subsidence determined from original LiDAR survey points and ground surface subsidence (50th %ile) estimated using LiDAR DEMs for Road (20-m buffer).

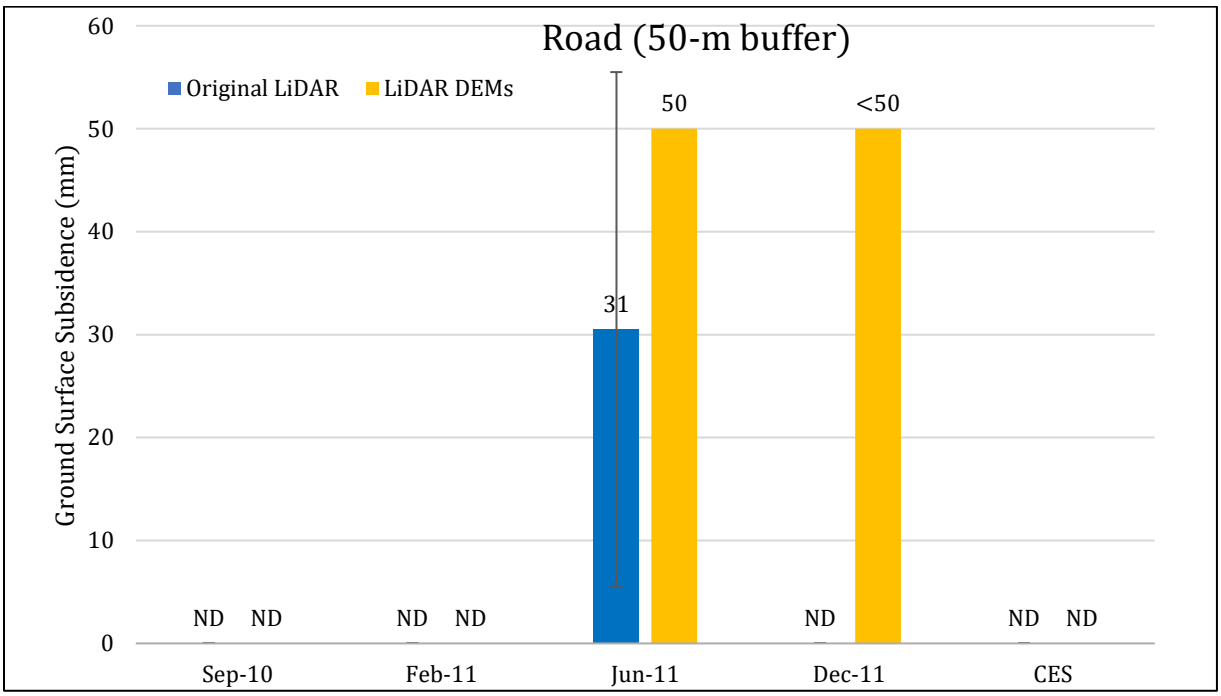

Figure 6: Comparison between ground surface subsidence determined from original LiDAR survey points and ground surface subsidence (50th %ile) estimated using LiDAR DEMs for Road (50-m buffer).

Note 2: The ground surface subsidence values determined from original LiDAR survey points are generally consistent with the ground surface subsidence values estimated using LiDAR DEMs for all earthquake events. The exception to this trend occurs for the Feb-11 earthquake for Patch A as the ground surface subsidence computed using the original LiDAR survey points is three times lower than the ground surface subsidence estimated using the LiDAR DEM (30 mm versus 100 mm, respectively).

Table 8a: Ejecta-Induced settlement for the top 20 m of the soil profile for Patch A (10-, 20-, and 50-m buffers) for the 50th %ile PGA, P_L=50%, and C_{FC}=0.13 using BI-2014, ZRB-2002, and I_C cutoff of 2.6.

Earthquake Event(s)	M_W	PGA (g)	Depth to Groundwater (m)	S_T (mm)	S_{V1D} (mm)	$S_{E,L}$ (mm)
Sep-10	7.1	0.22	0.5	ND	109±20	ND
Feb-11	6.2	0.57	0.5	30±75	225±50	-195±90
Jun-11	6.2	0.33	0.5	51±75	151±25	-100±79
Dec-11	6.1	0.24	0.5	ND	77±50	ND

Notes: S_T = Total settlement (Table 6); S_{V1D} = Average vertical settlement due to volumetric compression using Boulanger and Idriss (2014) (BI-2014), Zhang et al. (2002) (ZRB-2002) procedures and de Greef and Lengkeek (2018) thin-layer correction; $S_{E,L}$ = Ejecta-induced settlement as the difference between the LiDAR-based S_T and S_{V1D}.

Table 8b: Ejecta-Induced settlement for the top 20 m of the soil profile for Patch B (50-m buffer) for the 50th %ile PGA, P_L=50%, and C_{FC}=0.13 using BI-2014, ZRB-2002, and I_C cutoff of 2.6.

Earthquake Event(s)	M_W	PGA (g)	Depth to Groundwater (m)	S_T (mm)	S_{V1D} (mm)	$S_{E,L}$ (mm)
Sep-10	7.1	0.22	0.5	ND	146±20	ND
Feb-11	6.2	0.57	0.5	88±50	237±50	-149±71
Jun-11	6.2	0.33	0.5	36±50	176±25	-140±56
Dec-11	6.1	0.24	0.5	ND	115±50	ND

Notes: S_T = Total settlement (Table 6); S_{V1D} = Average vertical settlement due to volumetric compression using Boulanger and Idriss (2014) (BI-2014), Zhang et al. (2002) (ZRB-2002) procedures and de Greef and Lengkeek (2018) thin-layer correction; $S_{E,L}$ = Ejecta-induced settlement as the difference between the LiDAR-based S_T and S_{V1D}.

Table 8c: Ejecta-Induced settlement for the top 20 m of the soil profile for Road (20-m buffer) for the 50th %ile PGA, P_L=50%, and C_{FC}=0.13 using BI-2014, ZRB-2002, and I_c cutoff of 2.6.

Earthquake Event(s)	M_W	PGA (g)	Depth to Groundwater (m)	S_T (mm)	S_{V1D} (mm)	$S_{E,L}$ (mm)
Sep-10	7.1	0.22	0.5	ND	119±20	ND
Feb-11	6.2	0.57	0.5	ND	227±50	ND
Jun-11	6.2	0.33	0.5	43±25	156±25	-113±35
Dec-11	6.1	0.24	0.5	ND	89±50	ND

Notes: S_T = Total settlement (Table 6); S_{V1D} = Average vertical settlement due to volumetric compression using Boulanger and Idriss (2014) (BI-2014), Zhang et al. (2002) (ZRB-2002) procedures and de Greef and Lengkeek (2018) thin-layer correction; $S_{E,L}$ = Ejecta-induced settlement as the difference between the LiDAR-based S_T and S_{V1D}.

Table 8d: Ejecta-Induced settlement for the top 20 m of the soil profile for Road (50-m buffer) for the 50th %ile PGA, P_L=50%, and C_{FC}=0.13 using BI-2014, ZRB-2002, and I_c cutoff of 2.6.

Earthquake Event(s)	M_W	PGA (g)	Depth to Groundwater (m)	S_T (mm)	S_{V1D} (mm)	$S_{E,L}$ (mm)
Sep-10	7.1	0.22	0.5	ND	132±20	ND
Feb-11	6.2	0.57	0.5	ND	232±50	ND
Jun-11	6.2	0.33	0.5	31±25	168±25	-137±35
Dec-11	6.1	0.24	0.5	ND	102±50	ND

Notes: S_T = Total settlement (Table 6); S_{V1D} = Average vertical settlement due to volumetric compression using Boulanger and Idriss (2014) (BI-2014), Zhang et al. (2002) (ZRB-2002) procedures and de Greef and Lengkeek (2018) thin-layer correction; $S_{E,L}$ = Ejecta-induced settlement as the difference between the LiDAR-based S_T and S_{V1D}.

Note 3: The uncertainty for volumetric settlement was derived based on the sensitivity of volumetric settlement to PGA, C_{FC}, and P_L for each earthquake event for VsVp 57203 *Shirley Intermediate School* and CC LIQ 1 – CPT 5586 – *Vivian St* sites. Taking the 50th percentile as the baseline case, the minimum and maximum values corresponding to the difference between the 25th percentile and the 50th percentile and the 75th percentile and the 50th percentile were determined. The arithmetic mean of the range of the minimum and maximum difference was evaluated for each patch at the two sites. The maximum arithmetic mean for each earthquake event was rounded to the nearest five and used as the uncertainty value. Accordingly, the 1-D volumetric settlement uncertainties of ±20, ±50, ±25, and ±50 mm for the Sep-10, Feb-11, Jun-11, and Dec-11 earthquake events, respectively, were used for all sites in this study.

Table 9a: Coverage area and height of ejecta estimates for Patch A (10-, 20-, and 50-m buffers) using photographs.

Earthquake Event	$A_{E,thick}$ (m^2)	$H_{E,thick}$ (mm)	$A_{E,thin}$ (m^2)	$H_{E,thin}$ (mm)	A_T (m^2)
Sep-10	0	0	0	0	36.3
Feb-11	15.7	80-120	20.6	60-100	36.3
Jun-11	NA	NA	NA	NA	36.3
Dec-11	0	0	0	0	36.3

Notes: $A_{E,thick/thin}$ = Coverage area of thick/thin ejecta layers; $H_{E,thick/thin}$ = Lower-upper estimate of height of thick/thin ejecta layers; A_T = Total assessment area of a buffer being considered; Thin and thick layers correspond to light gray and dark gray colors of ejecta observed in aerial photographs.

Table 9b: Coverage area and height of ejecta estimates for Patch B (50-m buffer) using photographs.

Earthquake Event	$A_{E,thick}$ (m^2)	$H_{E,thick}$ (mm)	$A_{E,thin}$ (m^2)	$H_{E,thin}$ (mm)	A_T (m^2)
Sep-10	0	0	0	0	67.8
Feb-11	40.5	80-120	0	0	67.8
Jun-11	22.5	40-60	0	0	38.9*
Dec-11	0	0	0	0	67.8

Notes: $A_{E,thick/thin}$ = Coverage area of thick/thin ejecta layers; $H_{E,thick/thin}$ = Lower-upper estimate of height of thick/thin ejecta layers; A_T = Total assessment area of a buffer being considered; Thin and thick layers correspond to light gray and dark gray colors of ejecta observed in aerial photographs; * indicates reduction in A_T due to the presence of shadows.

Table 9c: Coverage area and height of ejecta estimates for Road (20-m buffer) using photographs.

EQ Event	$H_{E,prism/pyr}$ (mm)	$V_{E,prism+pyr}$ (m^3)	$H_{E,thick}$ (mm)	$A_{E,thick}$ (m^2)	$H_{E,thin}$ (mm)	$A_{E,thin}$ (m^2)	$H_{E,c}$ (mm)	$A_{E,c}$ (m^2)	A_T (m^2)
Sep-10	0	0	0	0	0	0	0	0	284
Feb-11	48-200	11.3-16.5	0	0	2-4	66.2	0	0	284
Jun-11	22-114	2.19-4.37	0	0	2-4	138	100-160	9.1	249*
Dec-11	0	0	0	0	0	0	0	0	284

Notes: $A_{E,c}$ = Coverage area of conically shaped ejecta layers; $H_{E,c}$ = Lower-upper estimate of height of conically shaped ejecta layers; $H_{E,prism/pyr}$ = Lower-upper estimate of ejecta height near the curb based on 2-4% cross slope of normal crown; $V_{E,prism+pyr}$ = Lower-upper estimate of total volume of prismatic- and pyramidal-shape ejecta; $A_{E,thin/thick}$ =Coverage area of thin/thick ejecta; $H_{E,\ thin/thick}$ = Lower-upper estimate of height of thin/thick ejecta layers; A_T= Total assessment area of a buffer being considered; * indicates reduction in A_T due to the presence of shadows.

Table 9d: Coverage area and height of ejecta estimates for Road (50-m buffer) using photographs.

EQ Event	$H_{E,prism/pyr}$ (mm)	$V_{E,prism+pyr}$ (m^3)	$H_{E,thick}$ (mm)	$A_{E,thick}$ (m^2)	$H_{E,thin}$ (mm)	$A_{E,thin}$ (m^2)	$H_{E,c}$ (mm)	$A_{E,c}$ (m^2)	A_T (m^2)
Sep-10	0	0	0	0	0	0	0	0	851
Feb-11	20-200	26.0-39.0	20-40	8.0	2-4	314	0	0	851
Jun-11	13-150	4.19-8.37	0	0	2-4	599	100-160	9.1	797*
Dec-11	0	0	0	0	0	0	0	0	851

Notes: $A_{E,c}$ = Coverage area of conically shaped ejecta layers; $H_{E,c}$ = Lower-upper estimate of height of conically shaped ejecta layers; $H_{E,prism/pyr}$ = Lower-upper estimate of ejecta height near the curb based on 2-4% cross slope of normal crown; $V_{E,prism+pyr}$ = Lower-upper estimate of total volume of prismatic- and pyramidal-shape ejecta; $A_{E,thin/thick}$ =Coverage area of thin/thick ejecta; $H_{E,\ thin/thick}$ = Lower-upper estimate of height of thin/thick ejecta layers; A_T= Total assessment area of a buffer being considered; * indicates reduction in A_T due to the presence of shadows.

Note 4: The values in Table 9 correspond to the coverage area of ejecta outlined in aerial photographs (Figures 30, 32, 34, 71, and 72) and the lower and upper estimates of ejecta height based on geometrical approximations, ground photographs (Figures 74 and 75), and EQC LDAT property inspection reports (Figure 73). The ejecta-induced settlement using photographs and engineering judgment, $S_{E,P}$, is estimated as

$$S_{E,P} = \frac{\sum_{i=1}^{a} A_{E,thick,i} * H_{E,thick,i} + \sum_{j=1}^{b} A_{E,thin,j} * H_{E,thin,j}}{A_T} + \frac{\frac{1}{3}\sum_{m=1}^{e} A_{E,cone,m} * H_{E,cone,m} + \frac{1}{2}\sum_{n=1}^{f} W_{E,prism,n} * H_{E,prism,n} * L_{E,prism,n}}{A_T} + \frac{\frac{1}{3}\sum_{p=1}^{g} W_{E,pyramid,p} * H_{E,pyramid} * L_{E,pyramid}}{A_T} = \frac{\sum_{i=1}^{a} V_{E,thick,i} + \sum_{j=1}^{b} V_{E,thin,j}}{A_T} + \frac{\sum_{m=1}^{e} V_{E,cone,m} + \sum_{n=1}^{f} V_{E,prism,n} + \sum_{p=1}^{g} V_{E,pyramid,p}}{A_T}$$

where

- $A_{E,thick,i}$ and $H_{E,thick,i}$ are the area and the height of a thick ejecta layer, respectively;
- $A_{E,thin,j}$ and $H_{E,thin,j}$ are the area and the height of a thin ejecta layer, respectively;
- $A_{E,cone,m}$ and $H_{E,cone,m}$ are the aerea and the height of a conically shaped ejecta, respectively;
- $W_{E,prism,n}$ and $L_{E,prism,n}$ are the width and the length of the coverage area of a prismatically shaped ejecta layer, respectively, and $H_{E,prism,n}$ is the height of a prism-like ejecta layer;
- $W_{E,pyr,p}$ and $L_{E,pyr,p}$ are the width and the length of the coverage area of a pyramid-like ejecta layer, respectively, and $H_{E,pyr,p}$ is the height of a pyramid-like ejecta layer;
- A_T is the total assessment area for a buffer being considered (Figure 1).

Table 10a: Ejecta-induced settlement estimates for Patches A and B based on photographs.

Earthquake Event	Patch A (10-, 20-, and 50-m buffers)		Patch B (50-m buffer)	
	$S_{E,P,lower}$ (mm)	$S_{E,P,upper}$ (mm)	$S_{E,P,lower}$ (mm)	$S_{E,P,upper}$ (mm)
Sep-10	0	0	0	0
Feb-11	69	109	48	72
Jun-11	NA	NA	23	35
Dec-11	0	0	0	0

Note: $S_{E,P,lower}$ and $S_{E,P,upper}$ correspond to lower and upper estimates of $S_{E,P}$, respectively.

Table 10b: Ejecta-induced settlement estimates for Road based on photographs.

Earthquake Event	Road (20-m buffer)		Road (50-m buffer)	
	$S_{E,P,lower}$ (mm)	$S_{E,P,upper}$ (mm)	$S_{E,P,lower}$ (mm)	$S_{E,P,upper}$ (mm)
Sep-10	0	0	0	0
Feb-11	40	59	32	48
Jun-11	11	22	7	14
Dec-11	0	0	0	0

Note: $S_{E,P,lower}$ and $S_{E,P,upper}$ correspond to lower and upper estimates of $S_{E,P}$, respectively.

Table 11a: Best final estimates of ejecta-induced settlement for Patches A and B.

EQ Event	Patch A (10-, 20-, and 50-m buffers)			Patch B (50-m buffer)		
	$S_{E,L}$ (mm)	$S_{E,P}$ (mm)	$S_{E,final}$ (mm)	$S_{E,L}$ (mm)	$S_{E,P}$ (mm)	$S_{E,final}$ (mm)
Sep-10	ND	0	0	ND	0	0
Feb-11	-195±90	89±20	90±20	-149±71	60±12	60±10
Jun-11	-100±79	NA	NA	-140±56	29±6	30±5
Dec-11	ND	0	0	ND	0	0

Notes: $S_{E,L}$ = Ejecta-induced settlement based on LiDAR data reported in Table 8; $S_{E,P}$ = Median ejecta-induced settlement for the range of values reported in Table 10; $S_{E,final}$ = Best final estimate of ejecta-induced settlement rounded to the nearest 5 mm; Final plus/minus values are also rounded to the nearest 5 mm; ND = Not determined.

Table 11b: Best final estimates of ejecta-induced settlement for Road.

Earthquake Event	Road (20-m buffer)			Road (50-m buffer)		
	$S_{E,L}$ (mm)	$S_{E,P}$ (mm)	$S_{E,final}$ (mm)	$S_{E,L}$ (mm)	$S_{E,P}$ (mm)	$S_{E,final}$ (mm)
Sep-10	ND	0	0	ND	0	0
Feb-11	ND	50±9	50±10	ND	40±8	40±10
Jun-11	-113±35	16.5±5.5	15±5	-137±35	10.5±3.5	10±5
Dec-11	ND	0	0	ND	0	0

Notes: $S_{E,L}$ = Ejecta-induced settlement based on LiDAR data reported in Table 8; $S_{E,P}$ = Median ejecta-induced settlement for the range of values reported in Table 10; $S_{E,final}$ = Best final estimate of ejecta-induced settlement rounded to the nearest 5 mm; Final plus/minus values are also rounded to the nearest 5 mm; ND = Not determined.

Note 5:

- $S_{E,final}$ is based solely on $S_{E,P}$ for all earthquake events due to the evident absence of ejecta for the Sep-10 and Dec-11 EQs and the negative $S_{E,L}$ values for the Feb-11 and Jun-11 EQs.
- The weight coefficients are based on the LiDAR error bands, LPI prediction error (Maurer et al. 2014[3]), presence of ejecta at the time of LiDAR surveys, and completeness of visual evidence (i.e., ground and aerial photographs and EQC LDAT property inspection reports for the site). The Randolph St site is in the apparent zone of higher ground surface subsidence for the Sep-10 EQ (i.e., the overestimate of the ground surface elevation by the Sep-10 LiDAR survey) and the apparent zone of lower ground surface subsidence for the Feb-11 EQ. The site is in the zone of slight to moderate LPI overprediction of liquefaction severity for the Sep-10 EQ and moderate to severe LPI overprediction for the Feb-11 EQ. The LDAT property inspection report and photographs are available for Patches A and B. The owner of the property where Patches A and B are located reported a "truck load of sand" for the Feb-11 EQ. No ejecta height measurements could be taken at this property due to the removal of ejecta at the time of the inspection. However, the ejecta height at nearby properties within the 50-m buffer was recorded as 300-400 mm. There are no ground photographs of the road.

Summary 1:

- **The best estimate of the ejecta-induced free-field ground settlement at the Randolph St site for the SEP 2010, JUN 2011, FEB 2011, and DEC 2011 earthquake is 0 mm, 90±20 mm, 30±5 mm, and 0 mm, respectively.**
- **The best estimate of the ejecta-induced free-field ground settlement of the road at the Randolph St site for the SEP 2010, FEB 2011, JUN 2011, and DEC 2011 earthquake is 0 mm, 50±10 mm, 15±5 mm, and 0 mm, respectively.**

[3] Maurer, B. W., Green, R. A., Cubrinovski, M., & Bradley, B. A. (2014). Evaluation of the Liquefaction Potential Index for Assessing Liquefaction Hazard in Christchurch, New Zealand. *Journal of Geotechnical and Geoenvironmental Engineering*, 140(7), 04014032-1-11. doi:10.1061/(asce)gt.1943-5606.0001117

Figure 7: Location of the site.

Figure 8: Position of the site relative to nearby buildings, vegetation, and free-face features.

Figure 9: Street view of the flat land.

Figure 10: Satellite image of the site taken in Dec 2004.

Figure 11: Satellite image of the site taken in Feb 2006.

Figure 12: Ground image showing road construction at the site in Dec 2007.

Figure 13: Satellite image of the site taken in Mar 2009.

Figure 14: Satellite image of the site taken in Oct 2009.

Figure 15: Satellite image of the site taken on Sep 3, 2010.

Figure 16: Satellite image of the site taken on Sep 5, 2010.

Figure 17: Satellite image of the site taken on Feb 15, 2011.

Figure 18: Satellite image of the site taken on Feb 26, 2011.

Figure 19: Satellite image of the site taken on Mar 8, 2011.

Figure 20: Satellite image of the site taken on Mar 28, 2011.

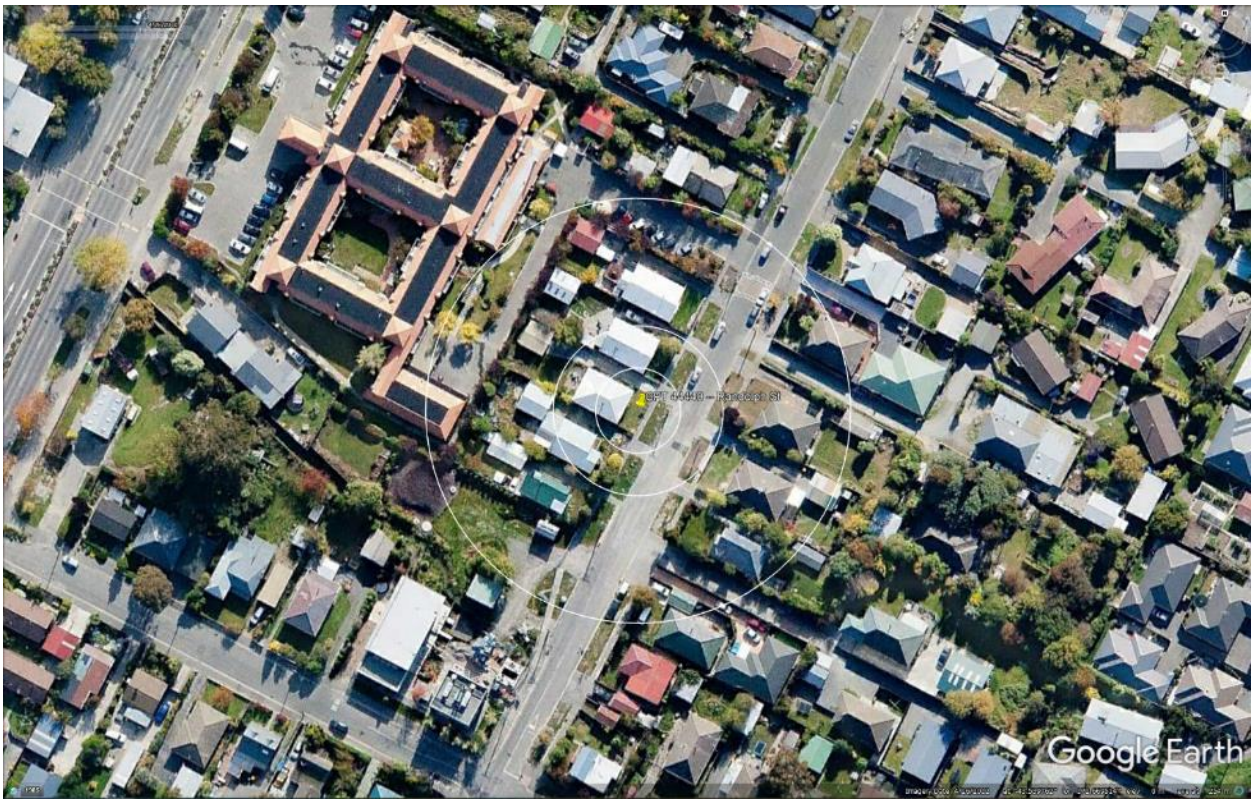

Figure 21: Satellite image of the site taken in Apr 2012.

Figure 22: Satellite image of the site taken in Mar 2013.

Figure 23: Satellite image of the site taken in Aug 2013.

Figure 24: Satellite image of the site taken in Aug 2014.

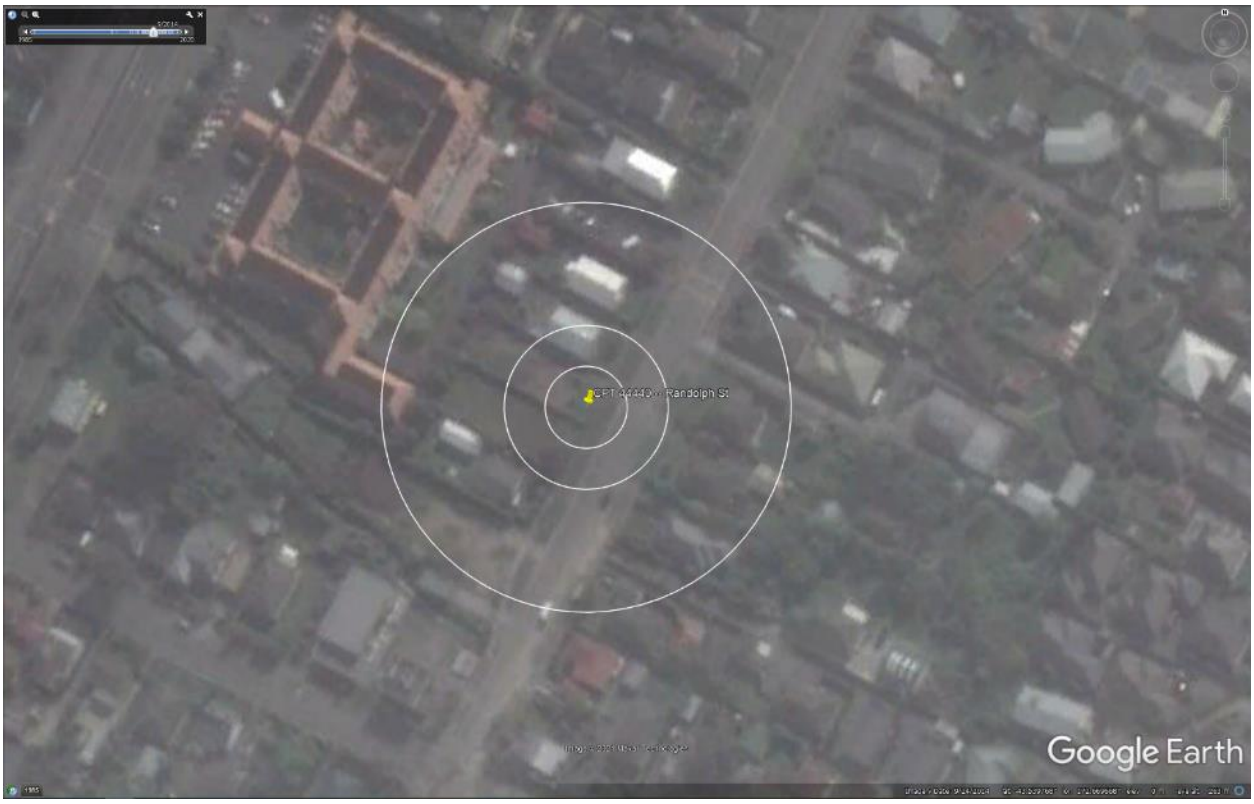

Figure 25: Satellite image of the site taken in Sep 2014.

Figure 26: Satellite image of the site taken in Jan 2015.

Figure 27: Satellite image of the site taken in July 2015.

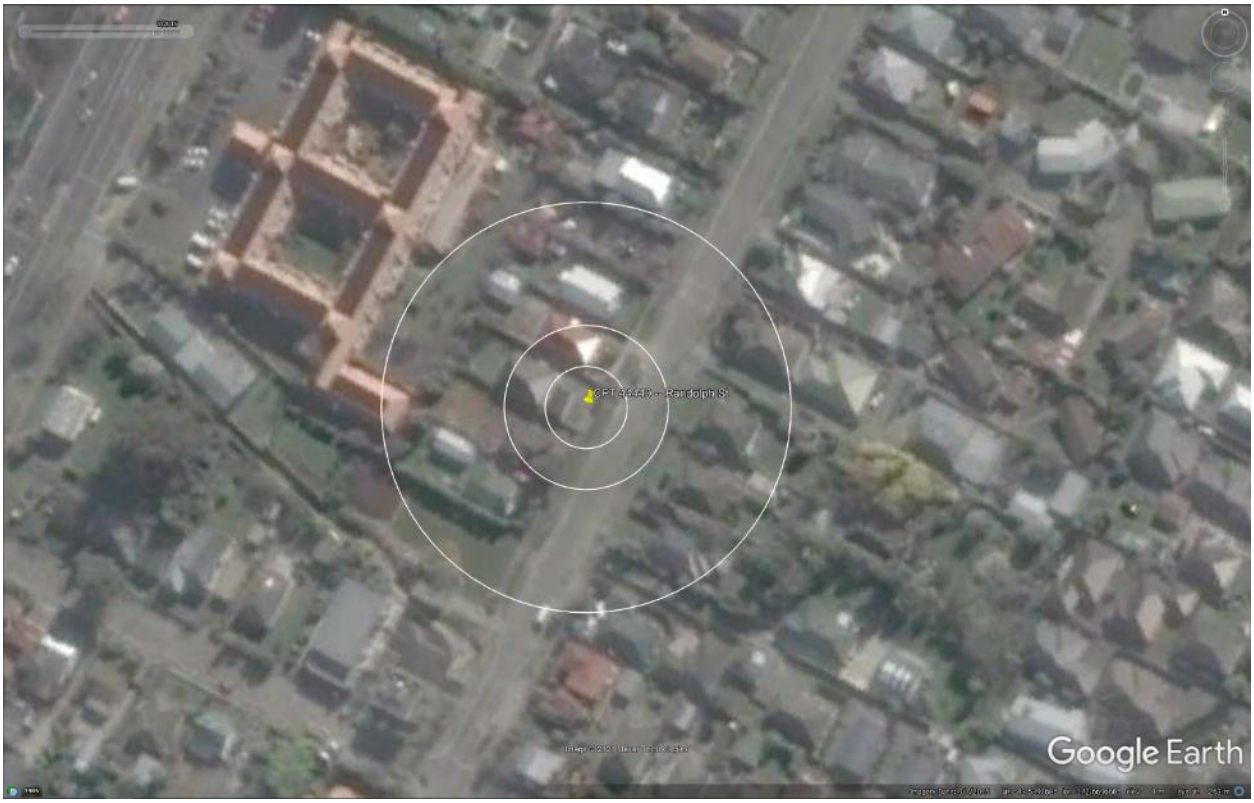

Figure 28: Satellite image of the site taken in Sep 2015.

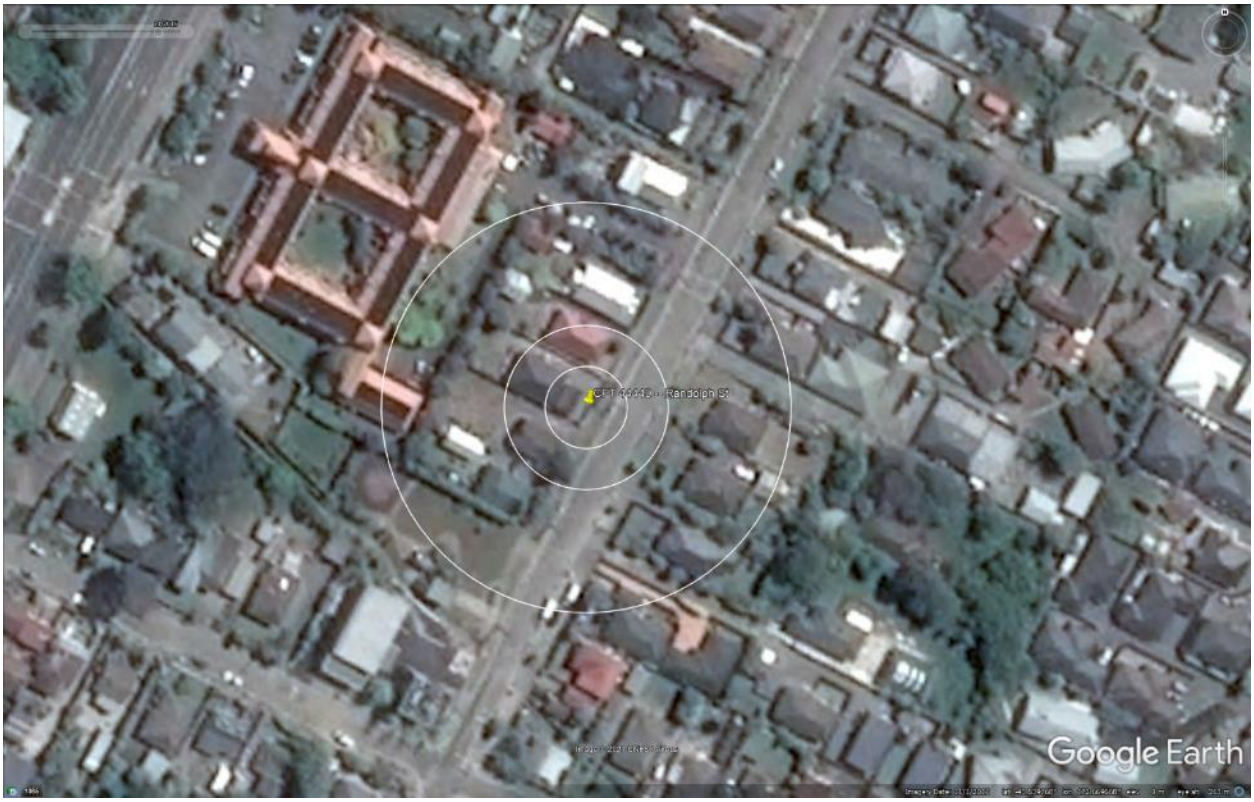

Figure 29: Satellite image of the site taken in Nov 2015.

Figure 30: Aerial photograph of the site taken on Sep 4, 2010.

Figure 31: Aerial photograph of the site taken on Feb 24, 2011.

Figure 32: Aerial photograph of the site taken on June 14-15, 2011.

Figure 33: Aerial photograph of the site taken on June 16, 2011.

Figure 34: Aerial photograph of the site taken on Dec 24, 2011.

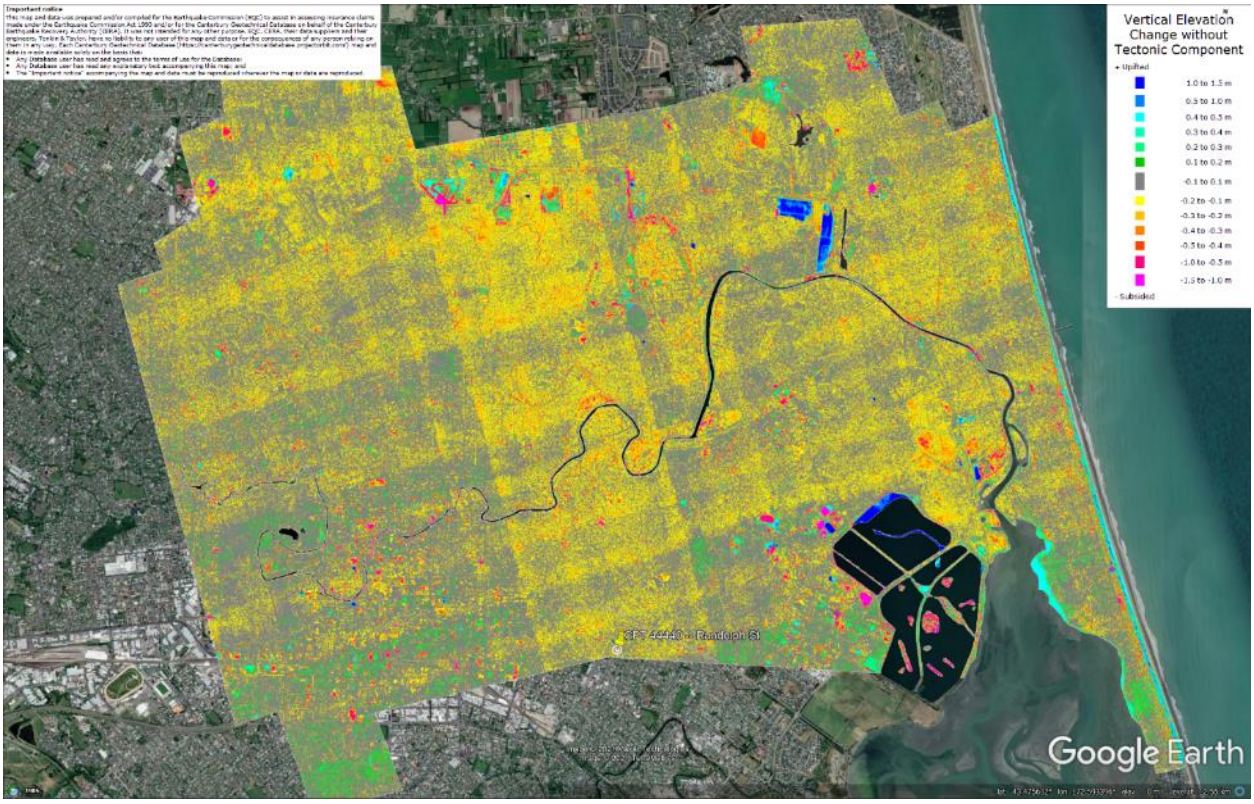

Figure 35: Vertical Ground Movements (Surface – Tectonic) for Sep 2010 Earthquake – the site is in the apparent zone of overestimated ground surface subsidence (i.e., Sep 2010 LiDAR flight error).

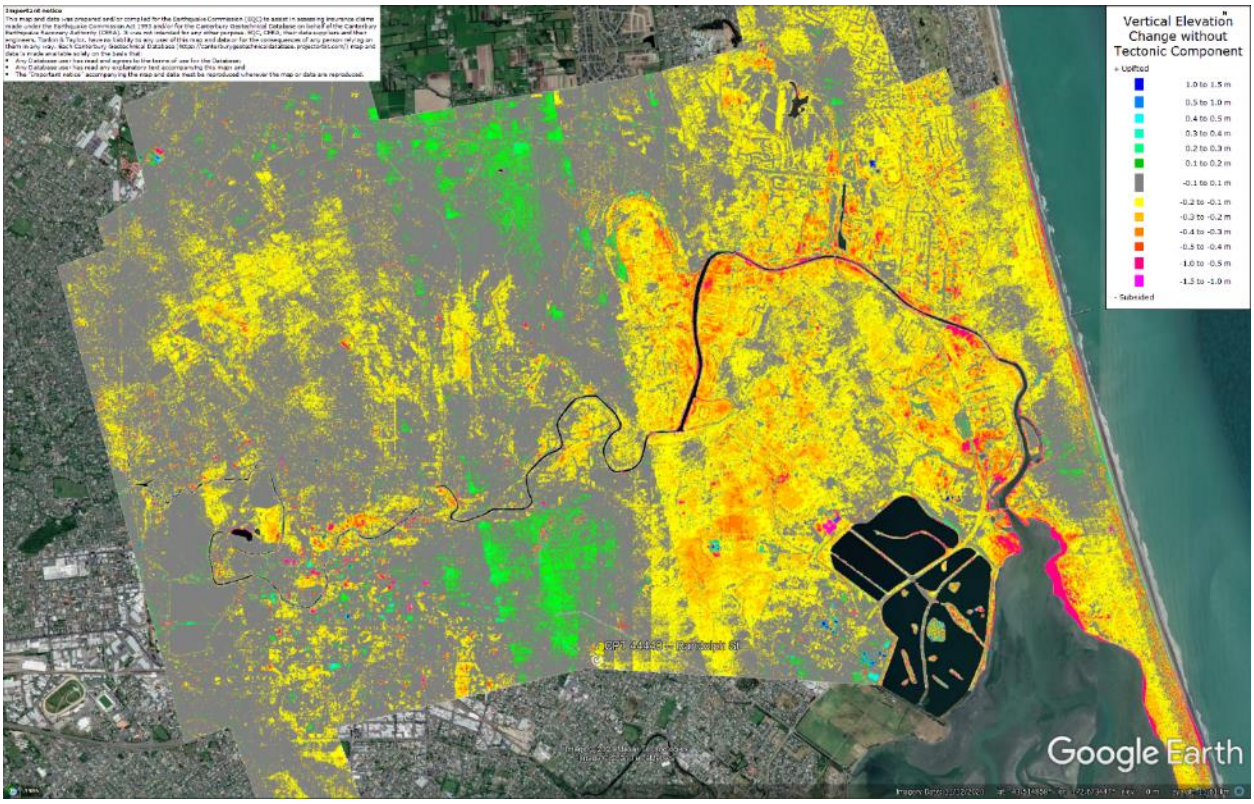

Figure 36: Vertical Ground Movements (Surface – Tectonic) for Feb 2011 Earthquake – the site is in the apparent zone of underestimated ground surface subsidence (i.e., Sep 2010 LiDAR flight error).

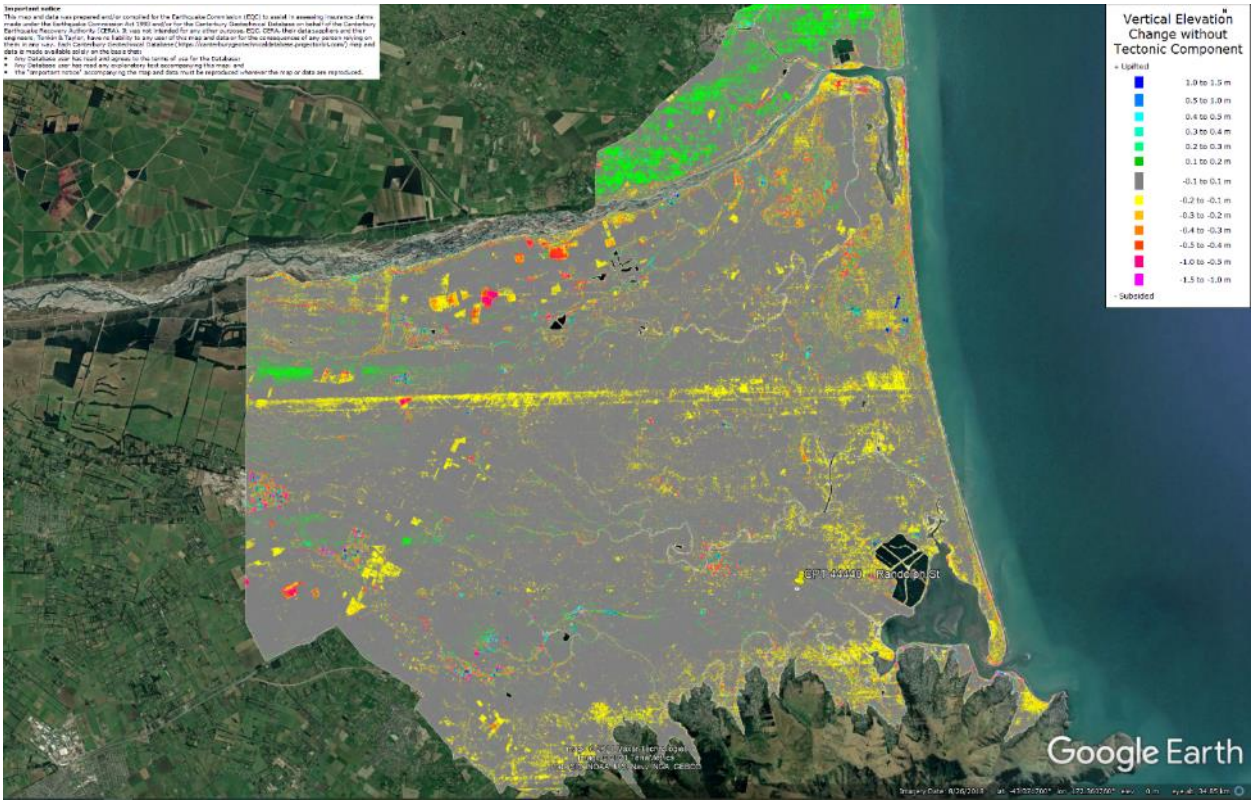

Figure 37: Vertical Ground Movements (Surface – Tectonic) for June 2011 Earthquake – the site is not in the apparent zone of overestimated/underestimated ground surface subsidence.

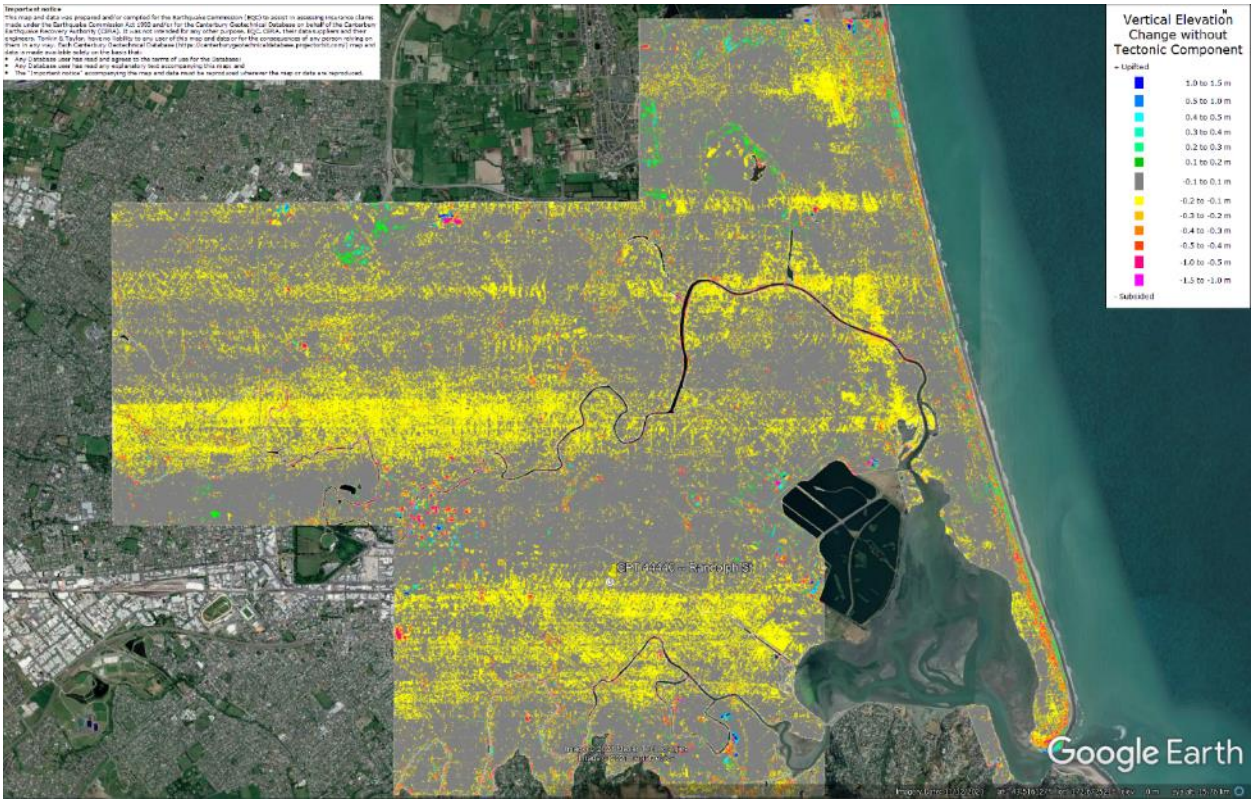

Figure 38: Vertical Ground Movements (Surface – Tectonic) for Dec 2011 Earthquake – the site is in the apparent zone of overestimated ground surface subsidence(i.e., Feb 2012 LiDAR flight error band).

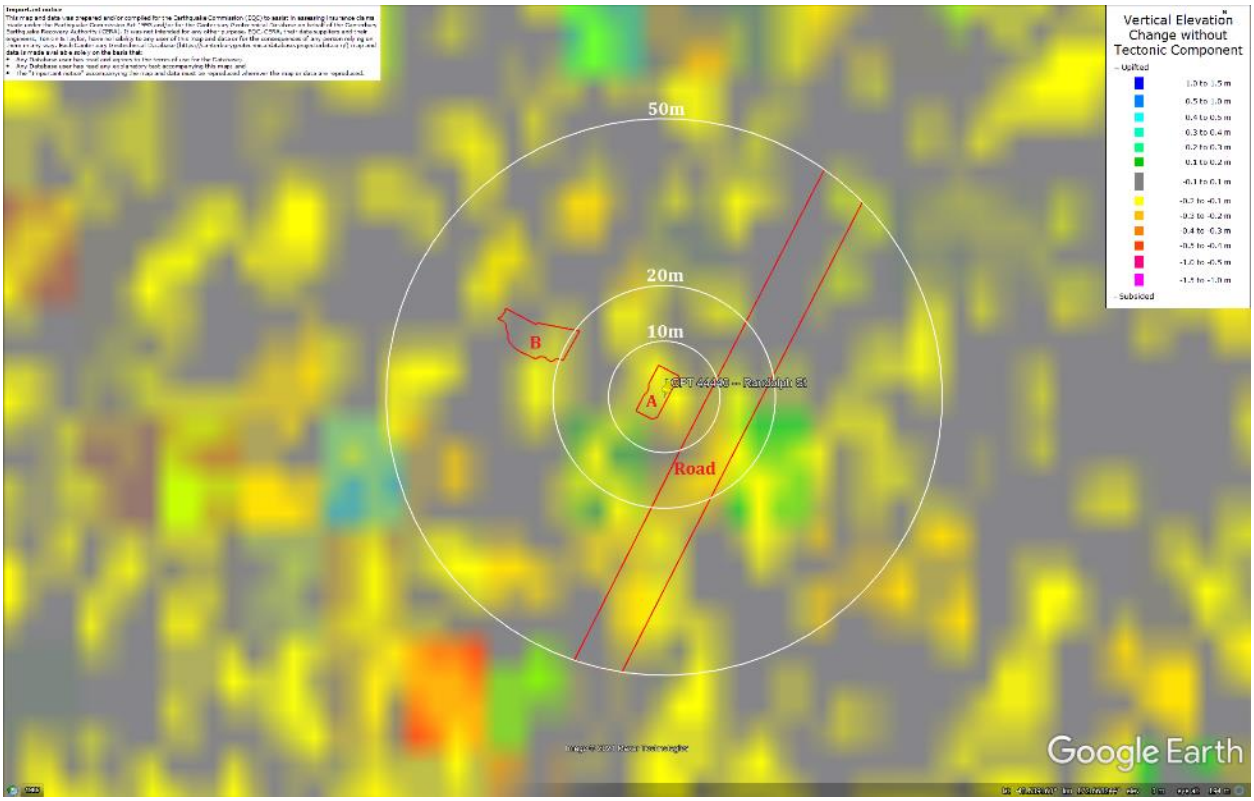

Figure 39: Ground surface subsidence without tectonic component for Sep 2010 Earthquake according to the LiDAR DEM.

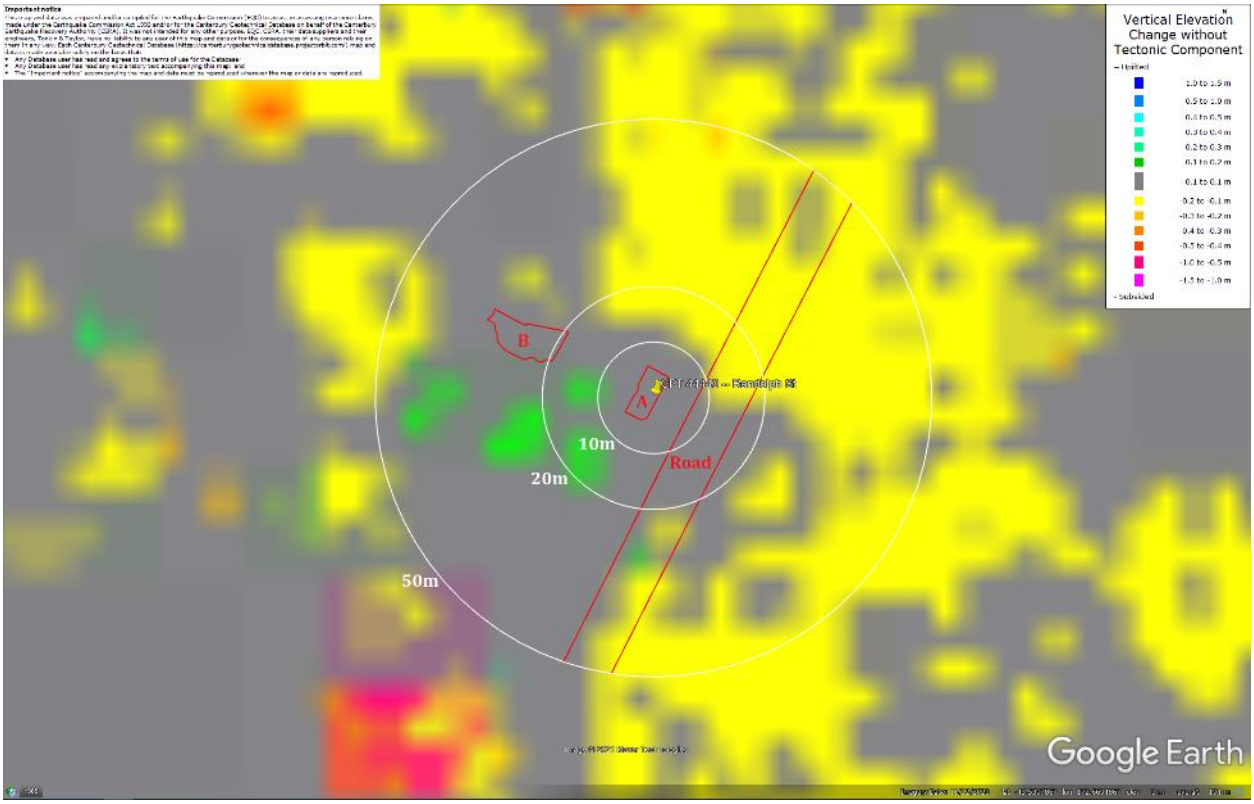

Figure 40: Ground surface subsidence without tectonic component for Feb 2011 Earthquake according to the LiDAR DEM.

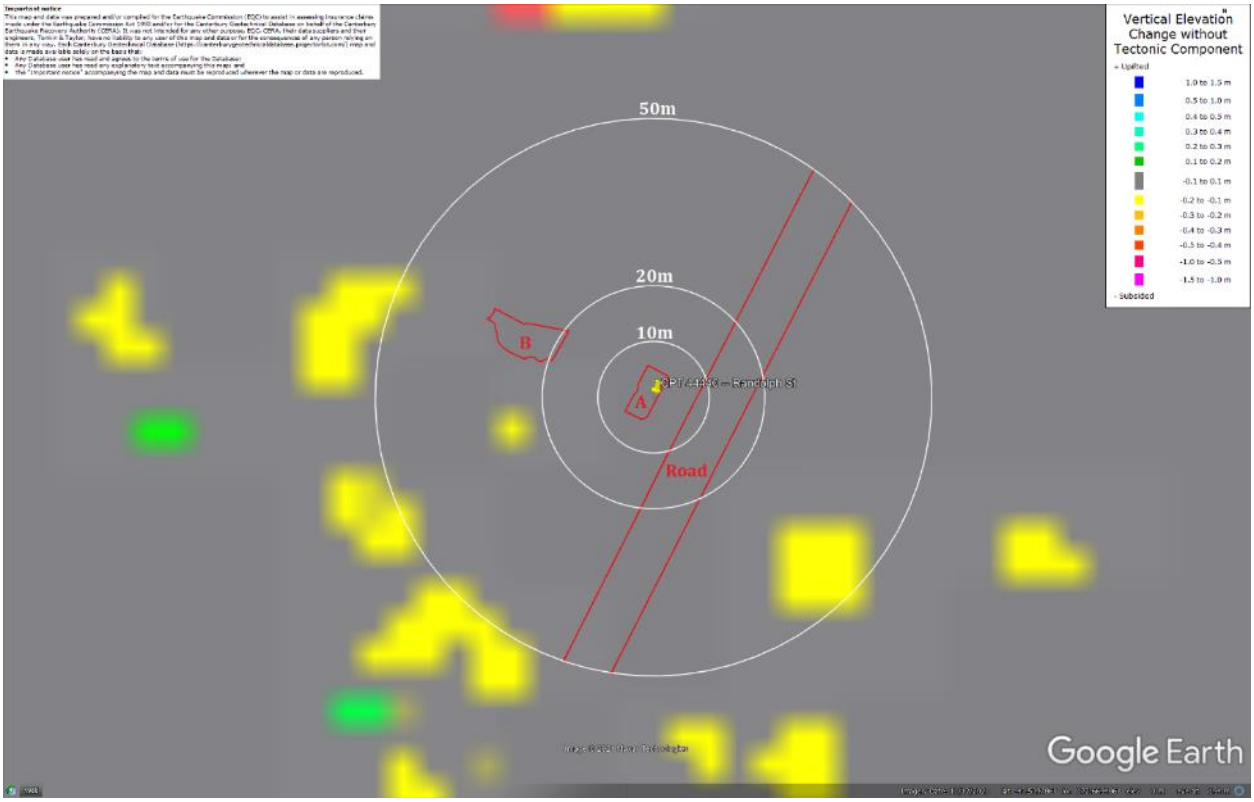

Figure 41: Ground surface subsidence without tectonic component for June 2011 Earthquake according to the LiDAR DEM.

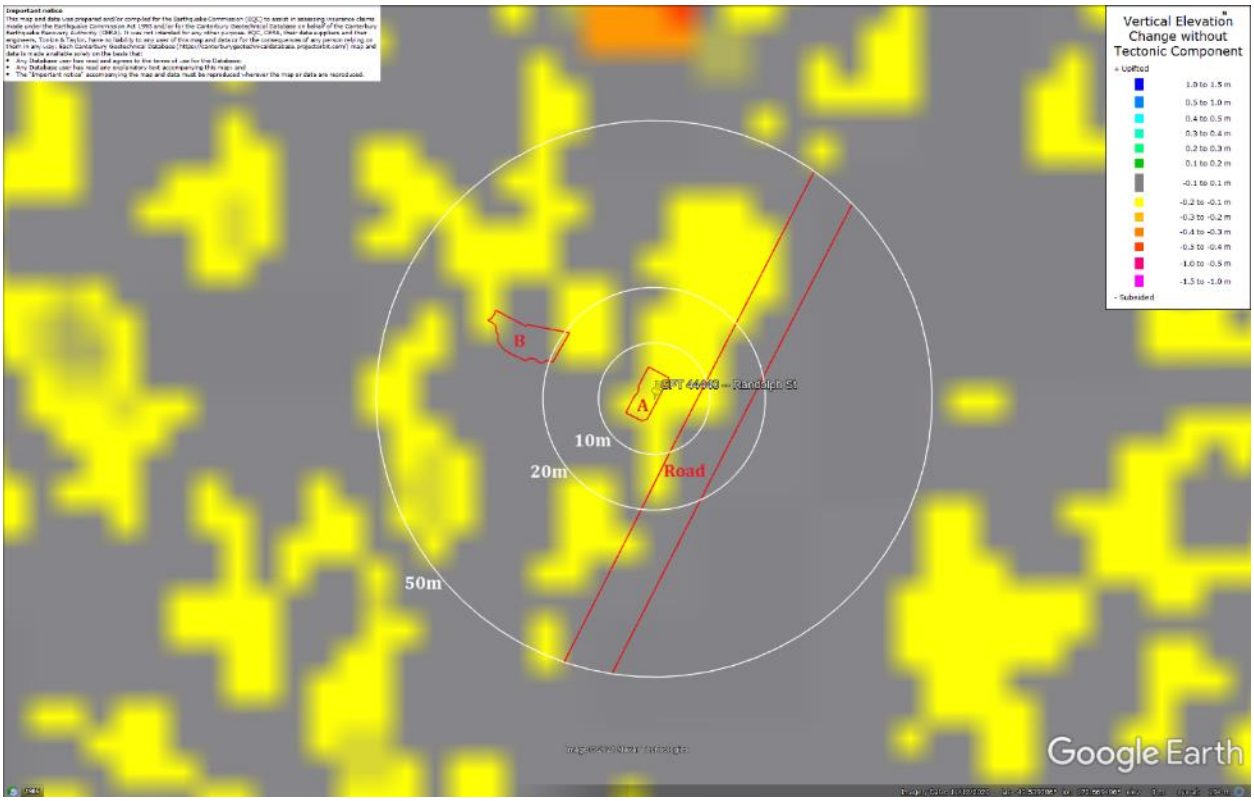

Figure 42: Ground surface subsidence without tectonic component for Dec 2011 Earthquake according to the LiDAR DEM.

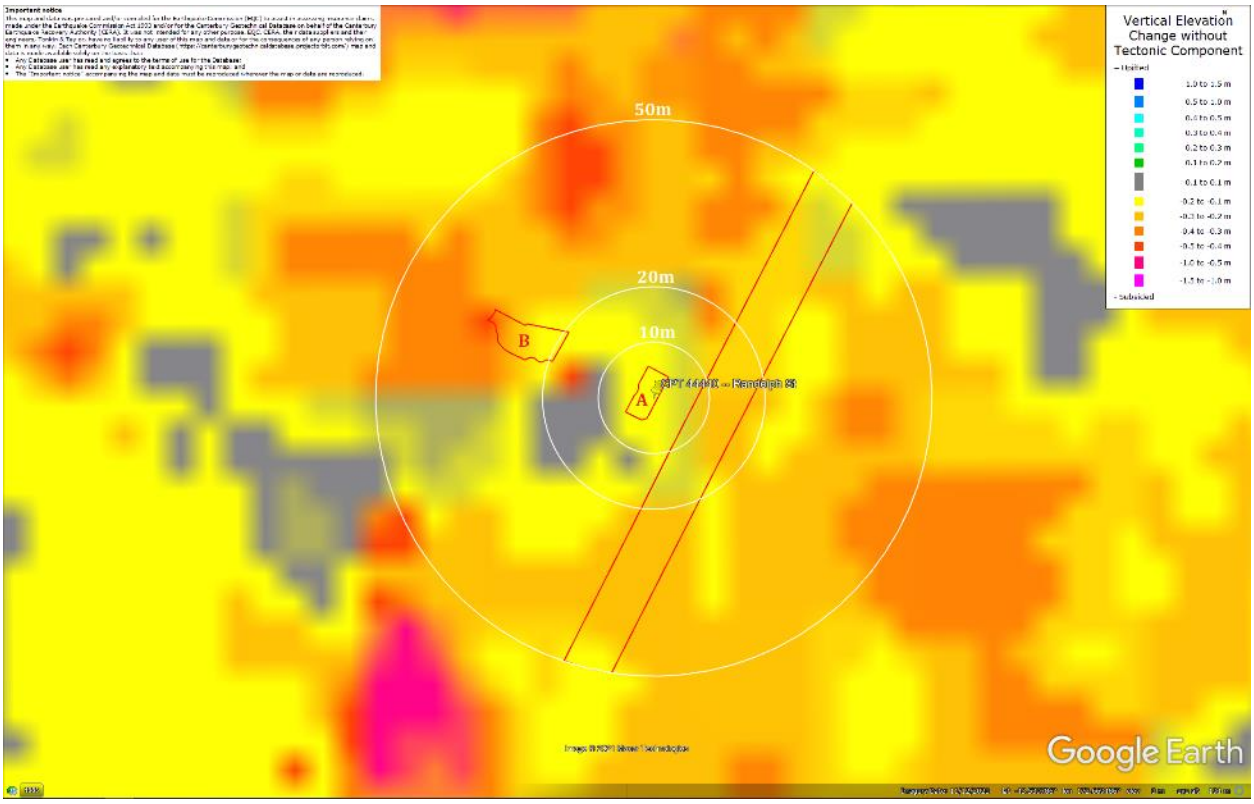

Figure 43: Ground surface subsidence without tectonic component for Canterbury Earthquake Sequence according to the LiDAR DEM.

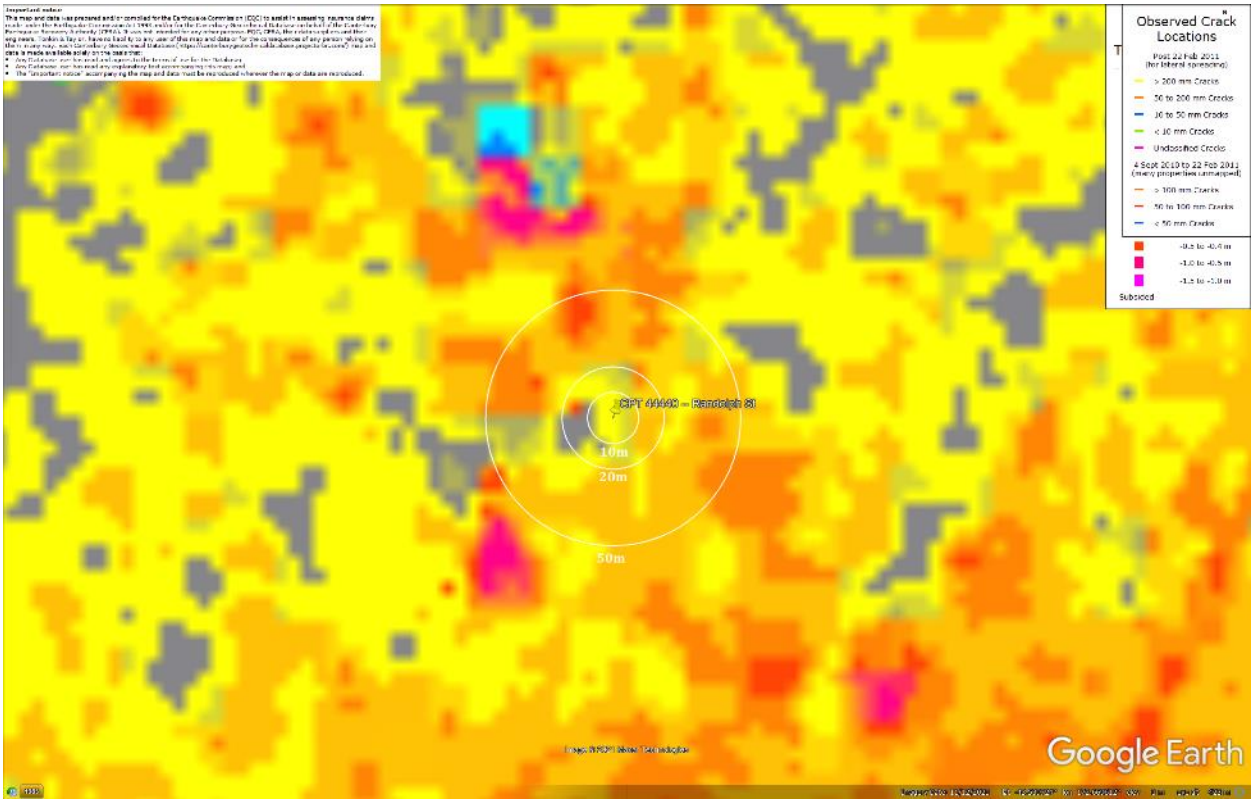

Figure 44: No lateral spreading for Canterbury Earthquake Sequence.

Figure 45: Vertical tectonic movements for Sep 2010 Earthquake.

Figure 46: Vertical tectonic movements for Feb 2011 Earthquake.

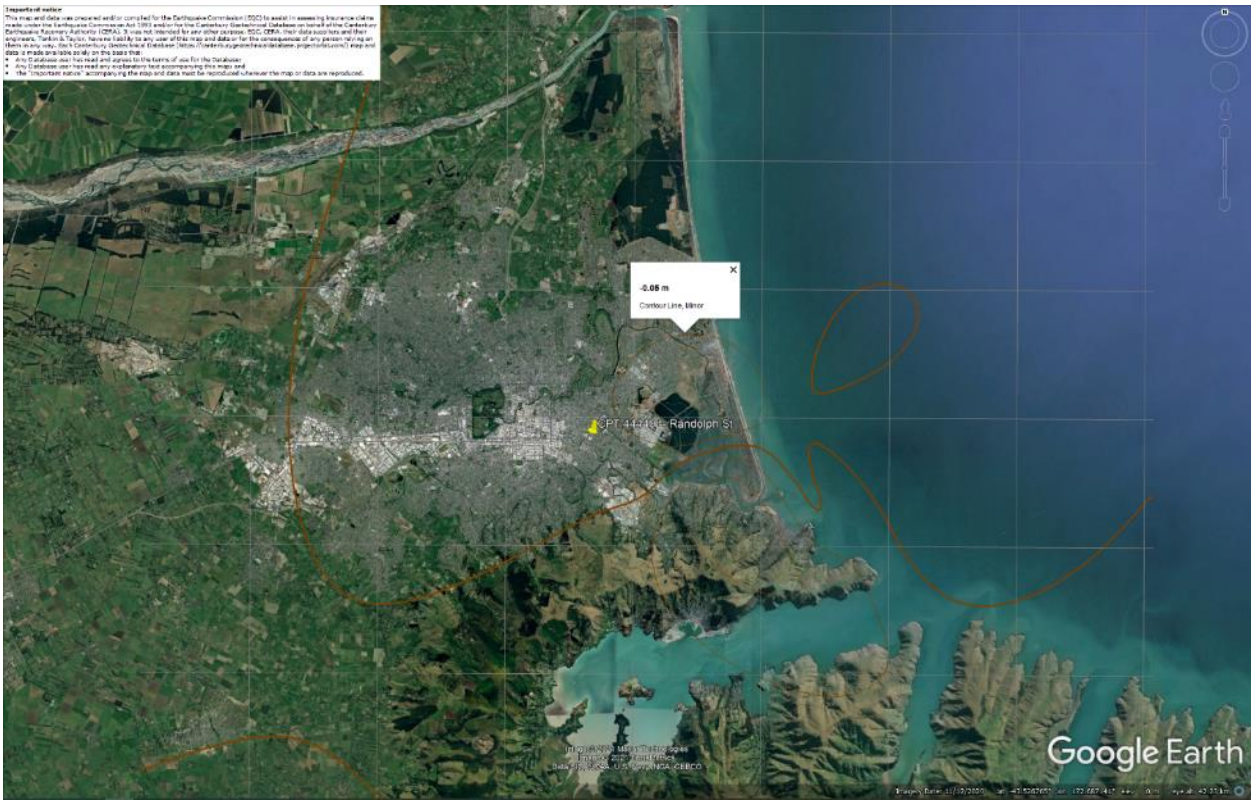

Figure 47: Vertical tectonic movements for June 2011 Earthquake.

Figure 48: Vertical tectonic movements for Dec 2011 Earthquake.

Figure 49: Vertical tectonic movements for Canterbury Earthquake Sequence.

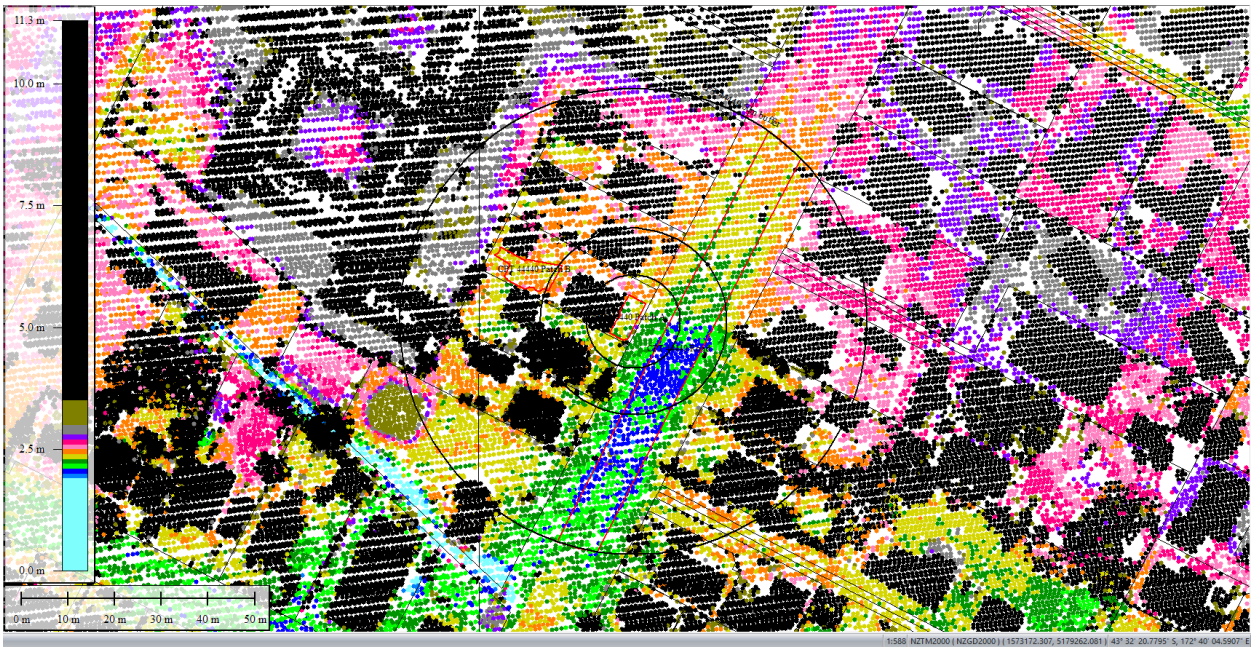

Figure 50: Sep 5, 2010 LiDAR survey.

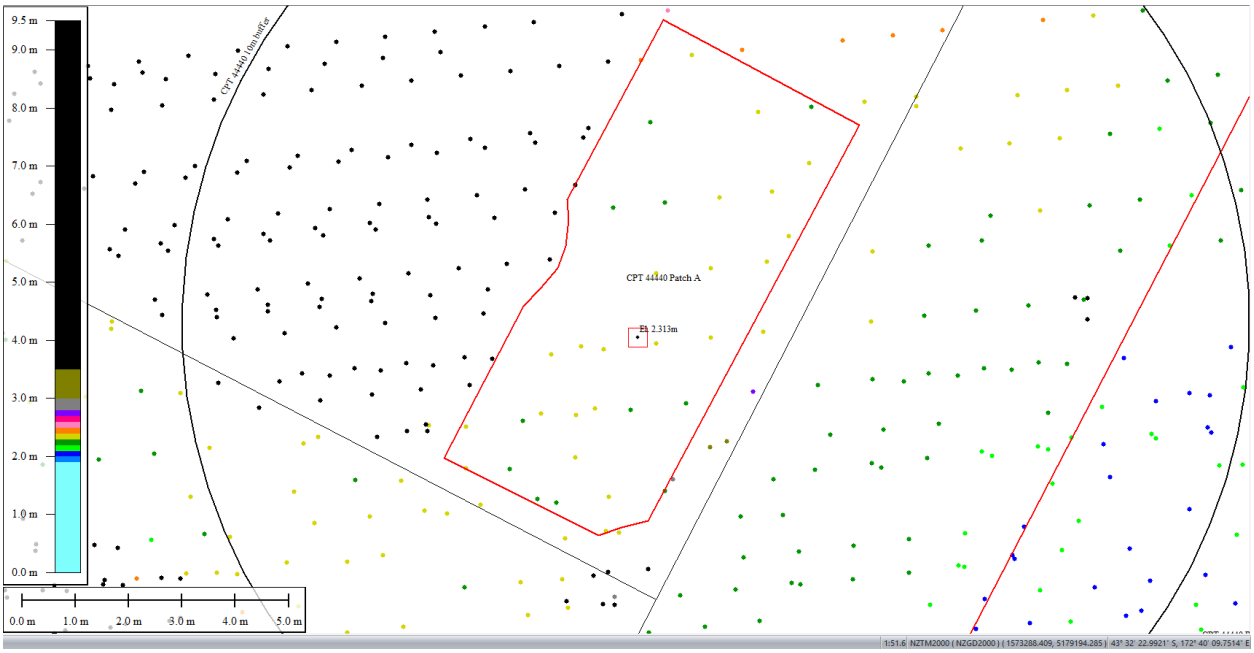

Figure 51: Ground surface elevation averaged over 10-m, 20-m, and 50-m buffers for Patch A for Sep 5, 2010 LiDAR survey.

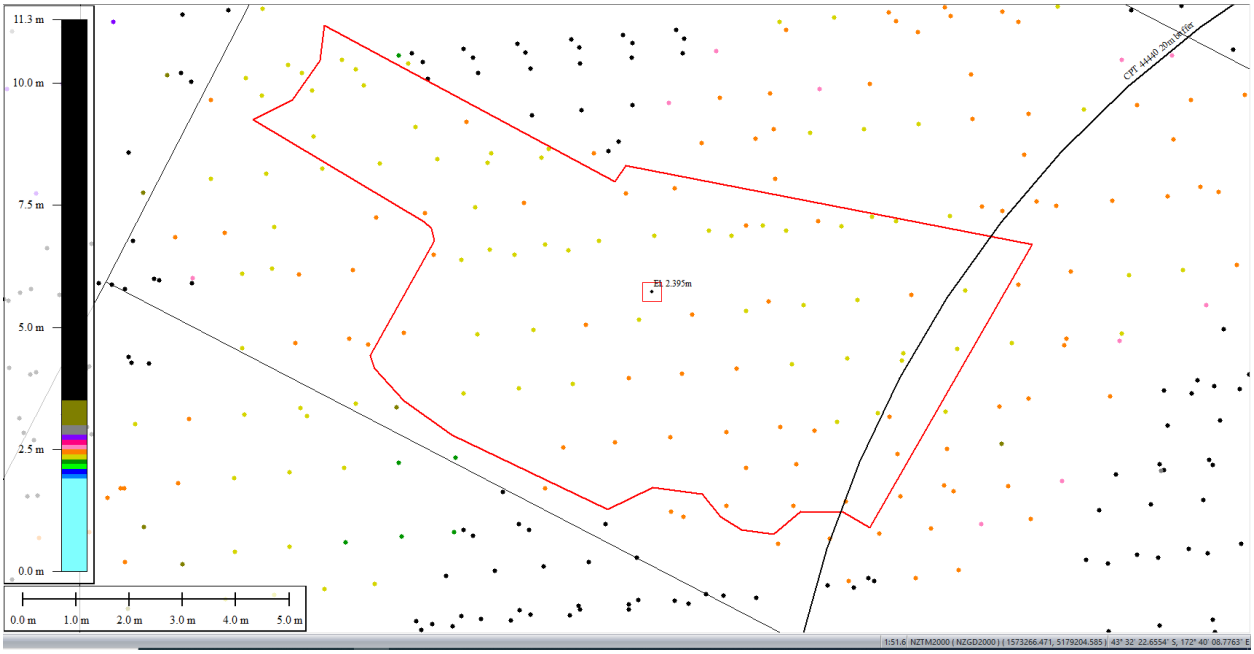

Figure 52: Ground surface elevation averaged over 50-m buffer for Patch B for Sep 5, 2010 LiDAR survey.

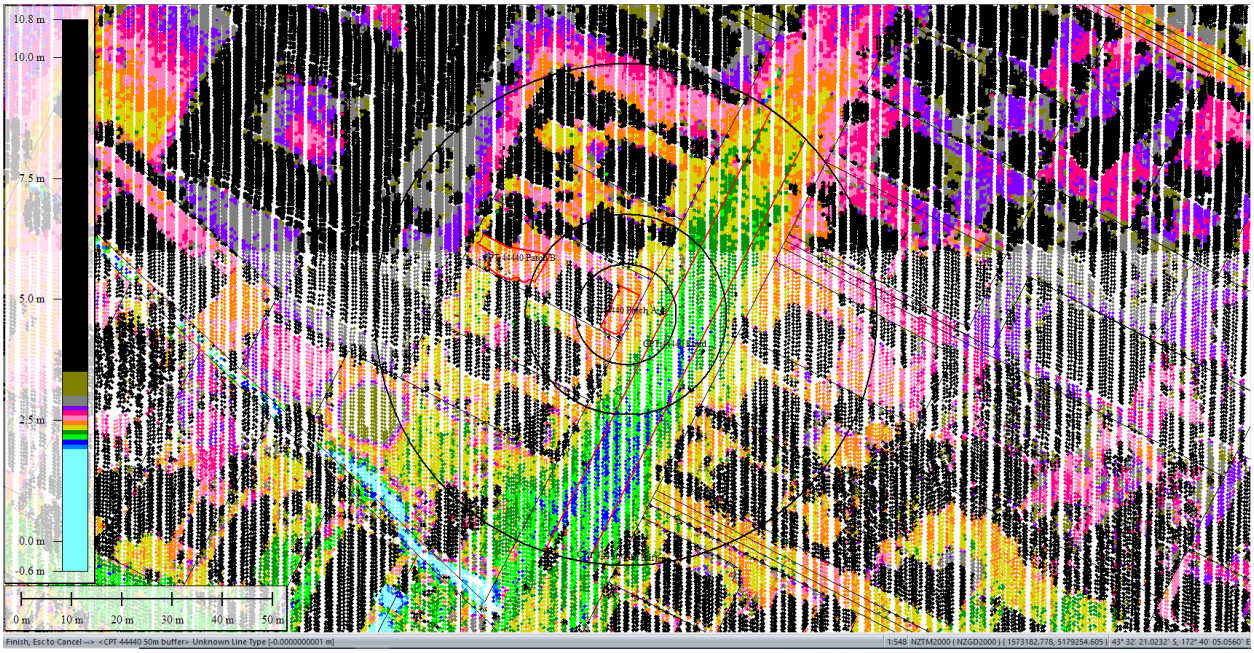

Figure 53: Mar 2011 LiDAR survey.

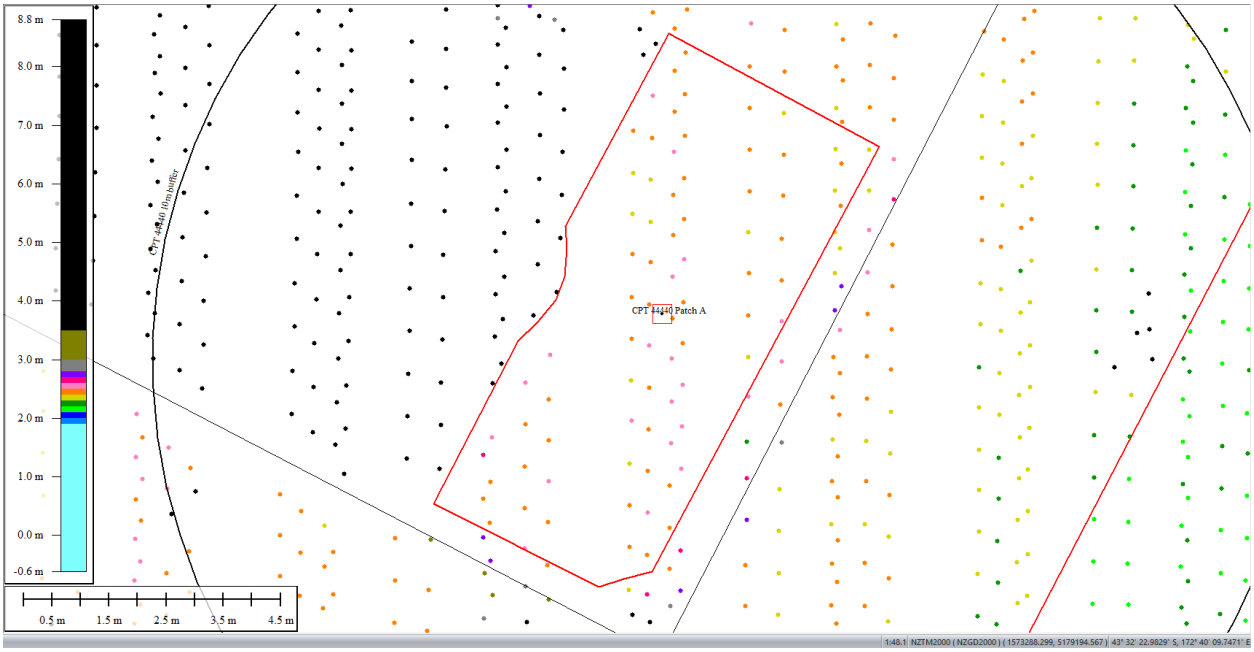

Figure 54: Ground surface elevation averaged over 10-m, 20-m, and 50-m buffers for Patch A for Mar 2011 LiDAR survey (el. 2.466m).

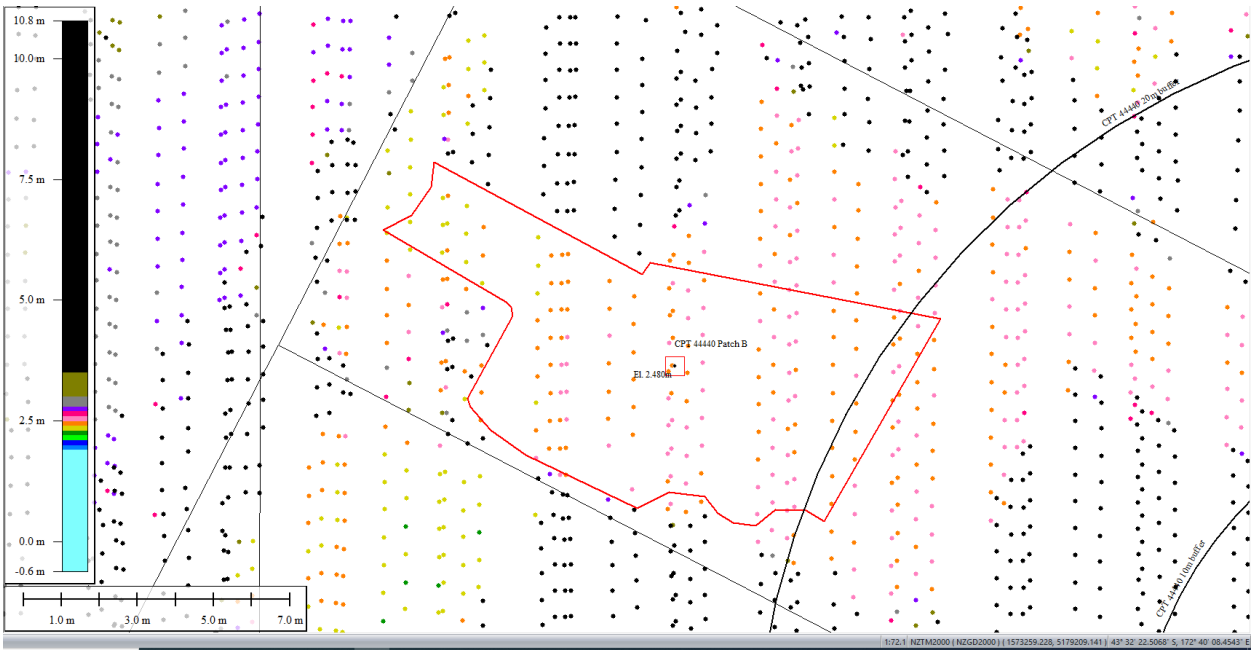

Figure 55: Ground surface elevation averaged over 50-m buffer for Patch B for Mar 2011 LiDAR survey.

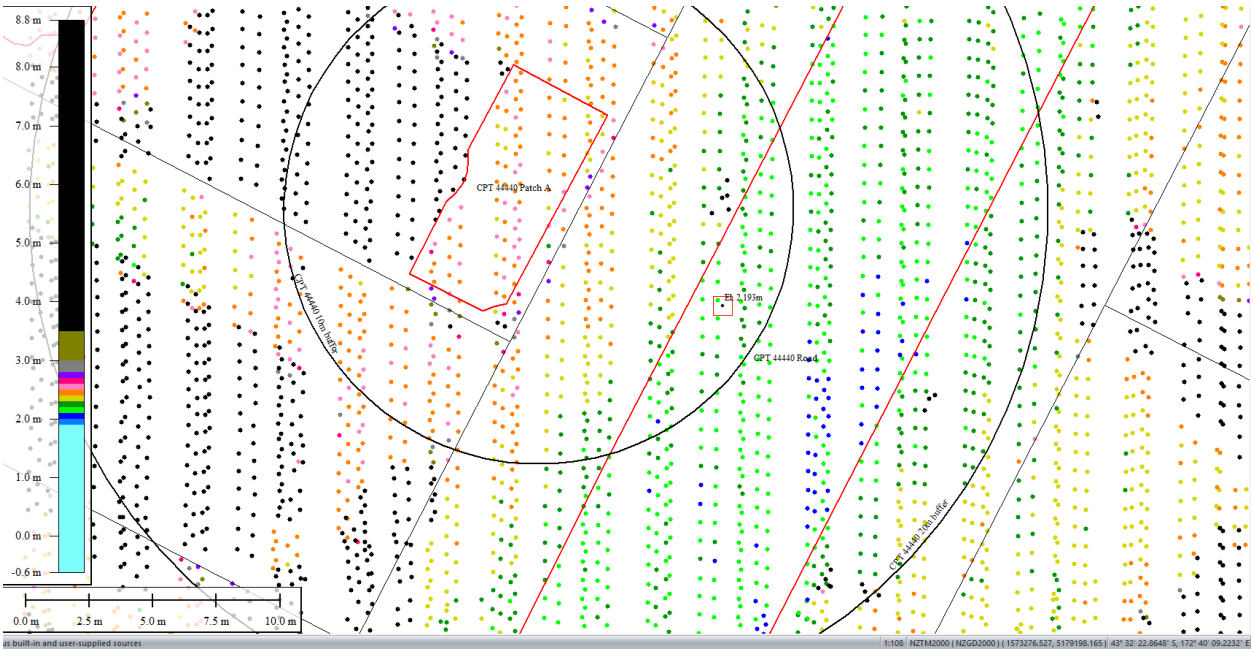

Figure 56: Ground surface elevation averaged over 10-m buffer for Road for Mar 2011 LiDAR survey.

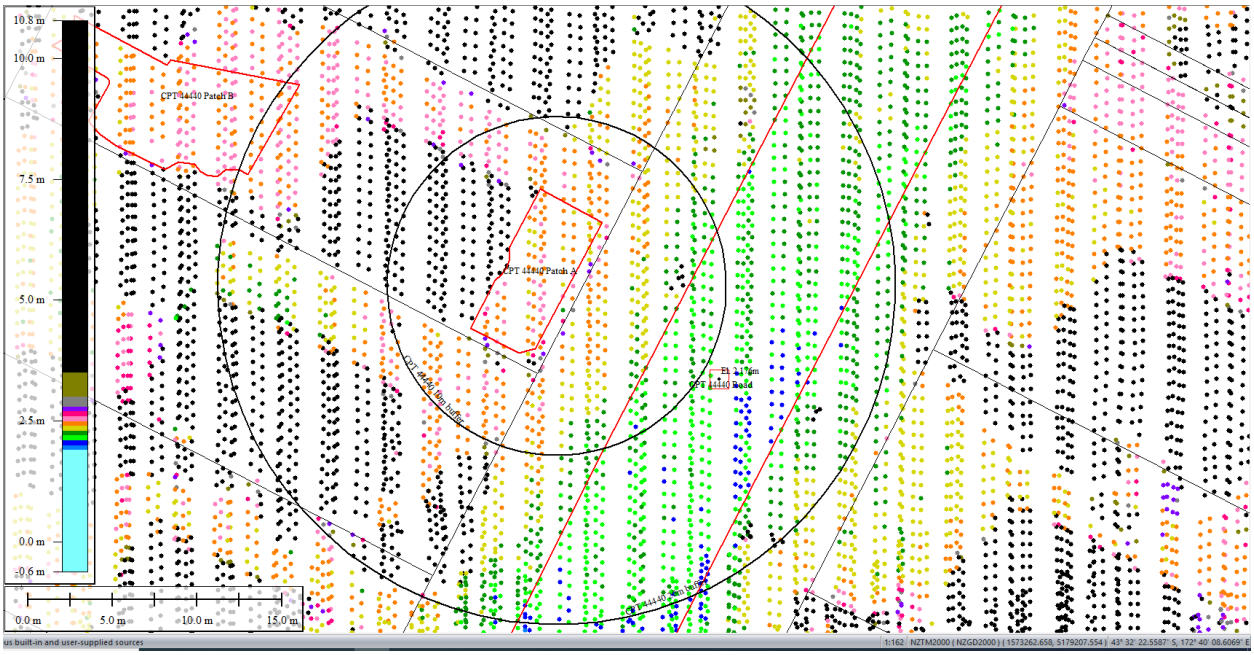

Figure 57: Ground surface elevation averaged over 20-m buffer for Road for Mar 2011 LiDAR survey.

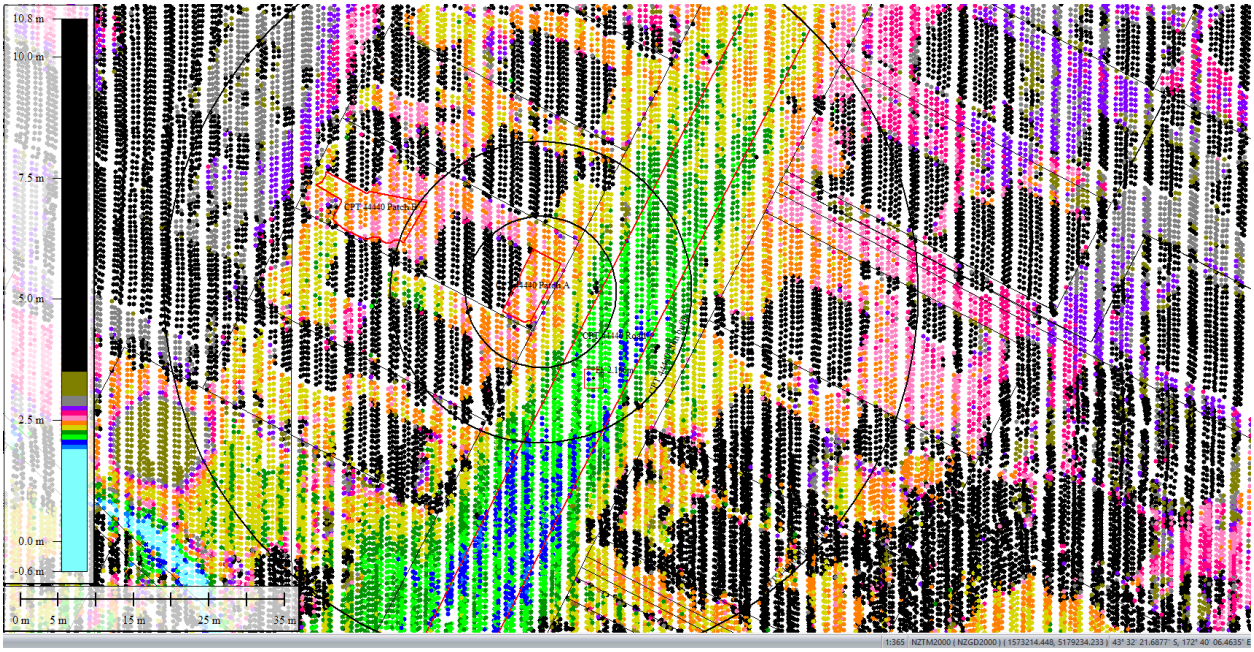

Figure 58: Ground surface elevation averaged over 50-m buffer for Road for Mar 2011 LiDAR survey.

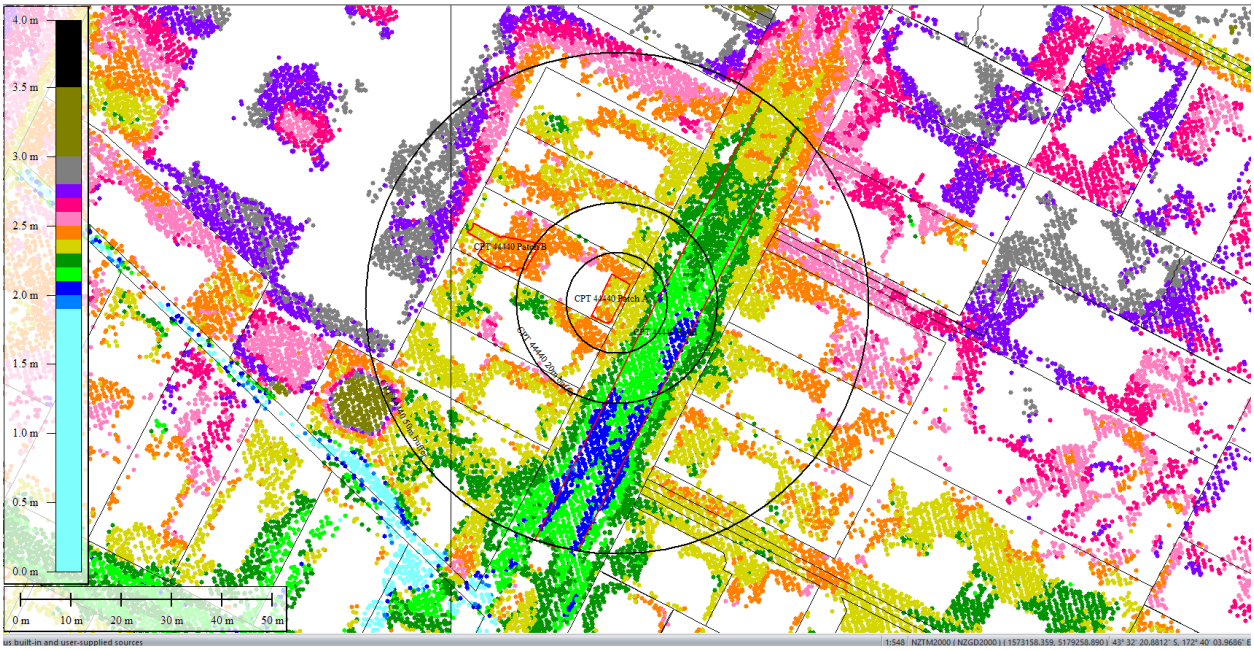

Figure 59: May 2011 LiDAR survey.

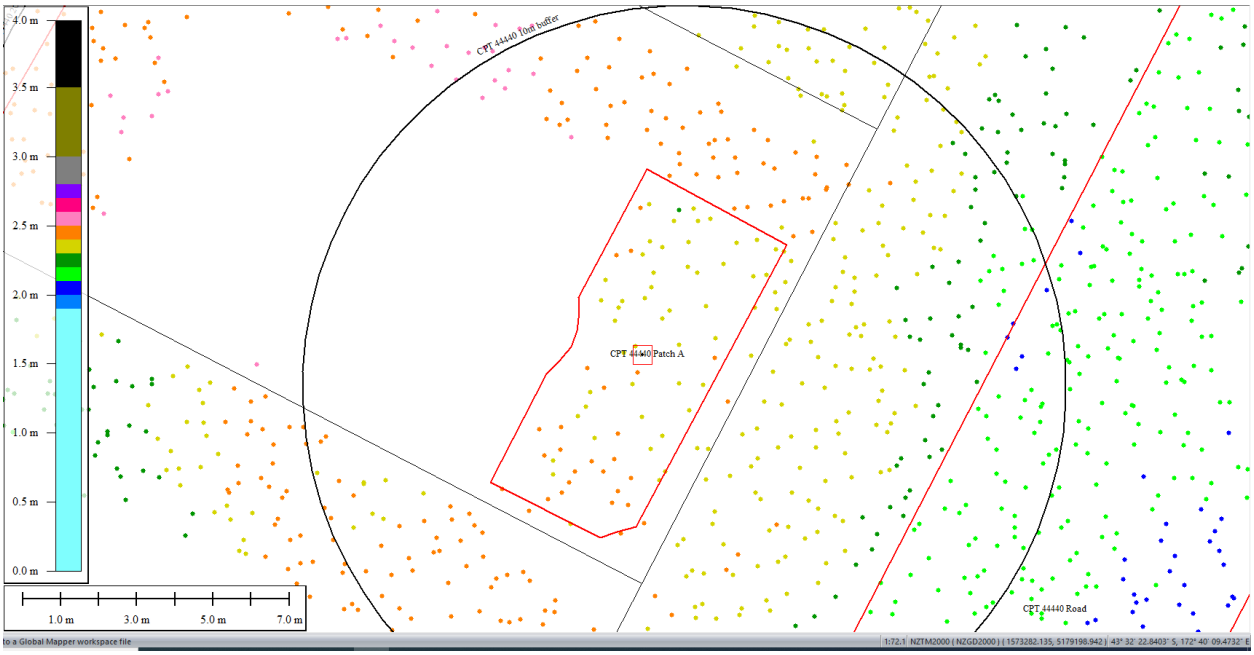

Figure 60: Ground surface elevation averaged over 10-m, 20-m, and 50-m buffers for Patch A for May 2011 LiDAR survey.

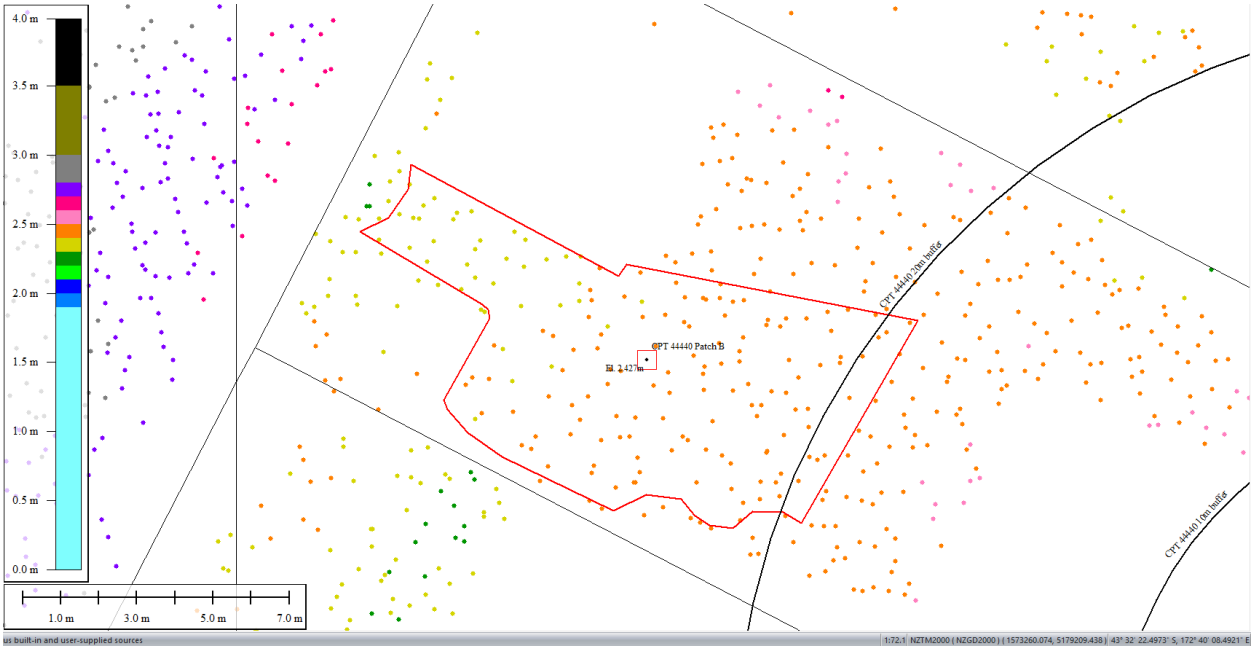

Figure 61: Ground surface elevation averaged over 50-m buffer for Patch B for May 2011 LiDAR survey.

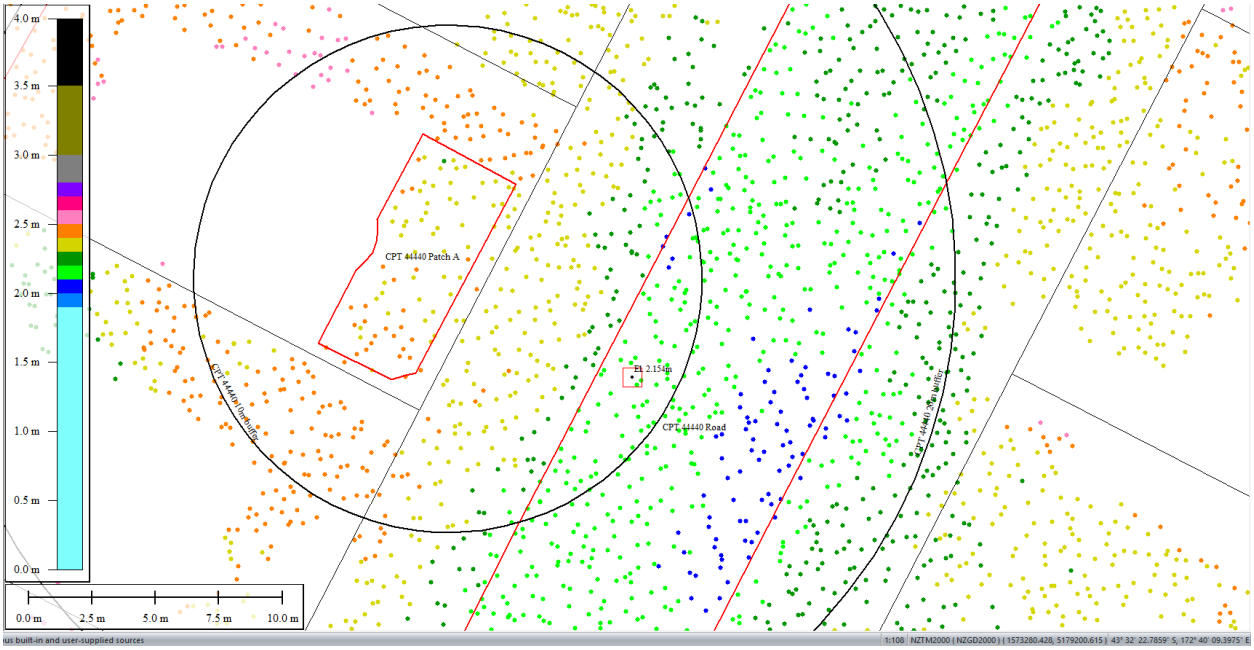

Figure 62: Ground surface elevation averaged over 10-m buffer for Road for May 2011 LiDAR survey.

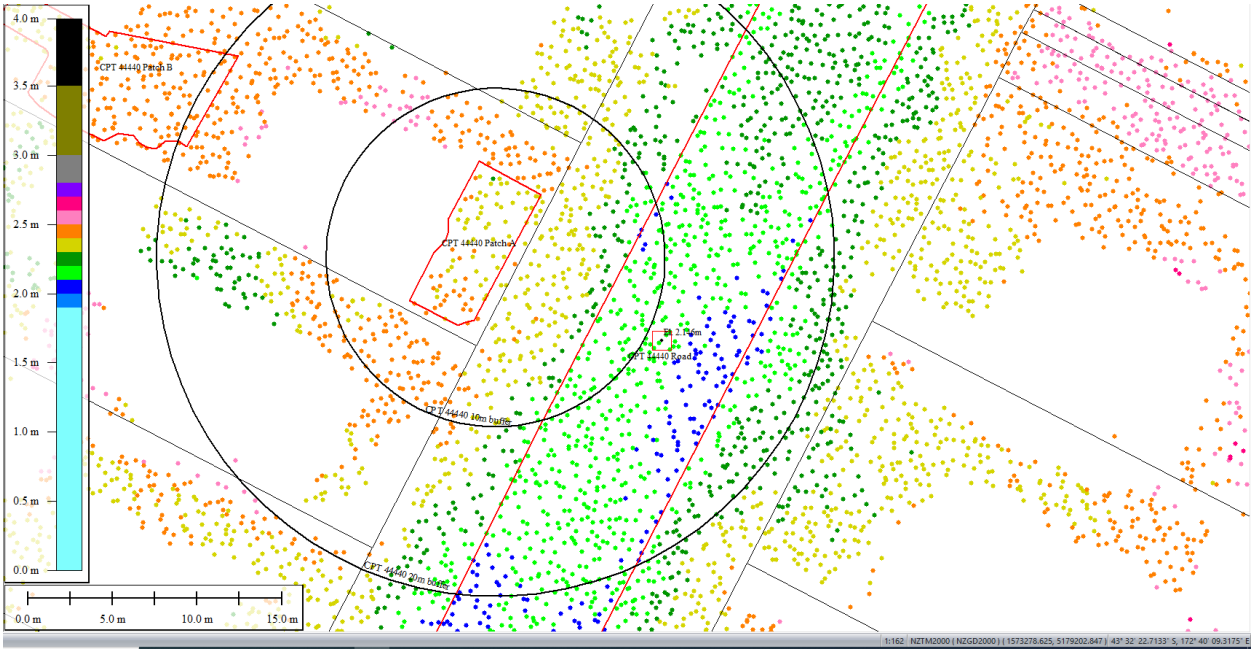

Figure 63: Ground surface elevation averaged over 20-m buffer for Road for May 2011 LiDAR survey.

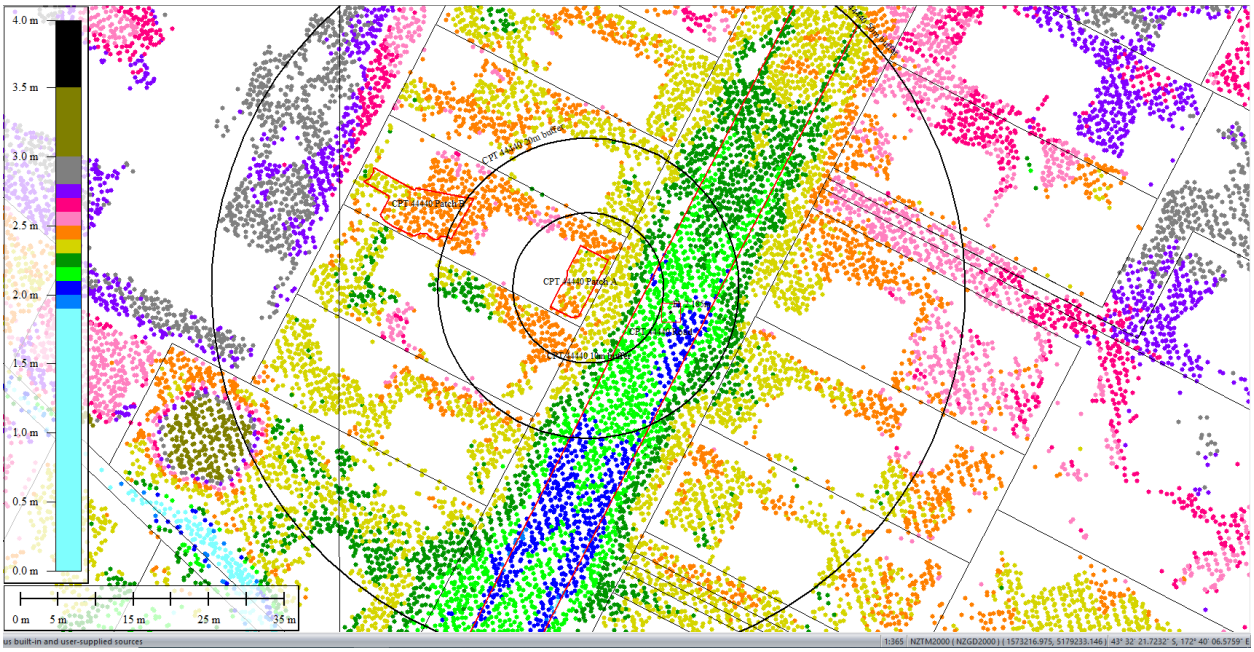

Figure 64: Ground surface elevation averaged over 50-m buffer for Road for May 2011 LiDAR survey.

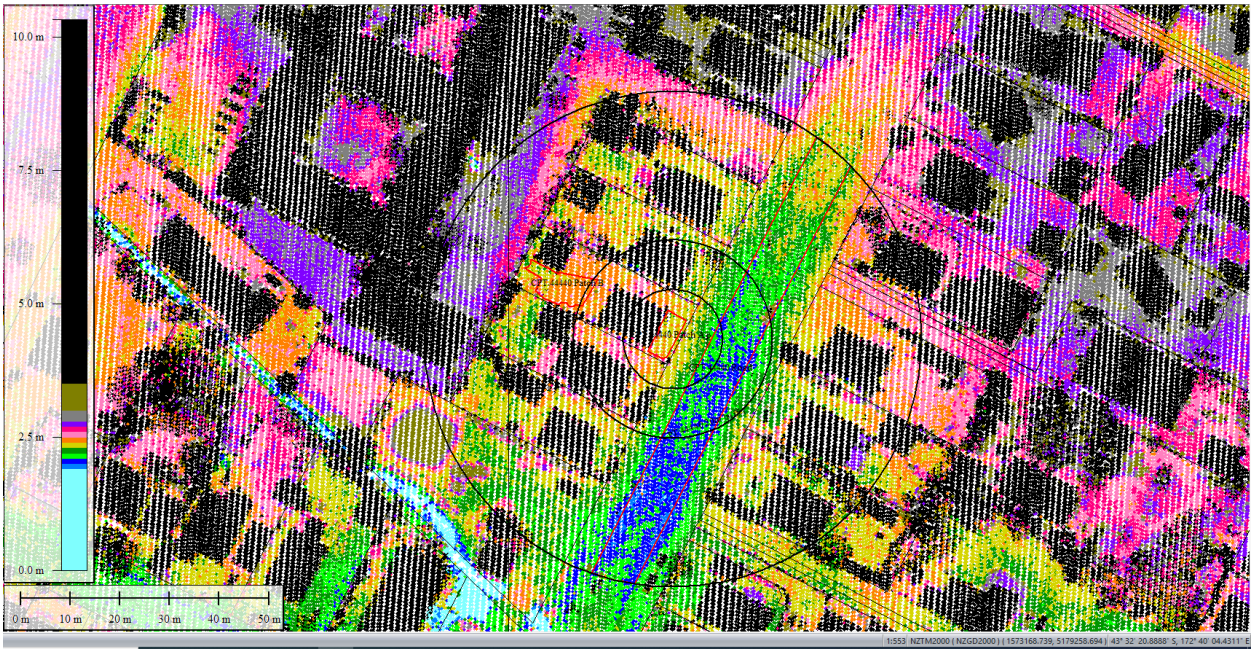

Figure 65: Sep 2011 LiDAR survey.

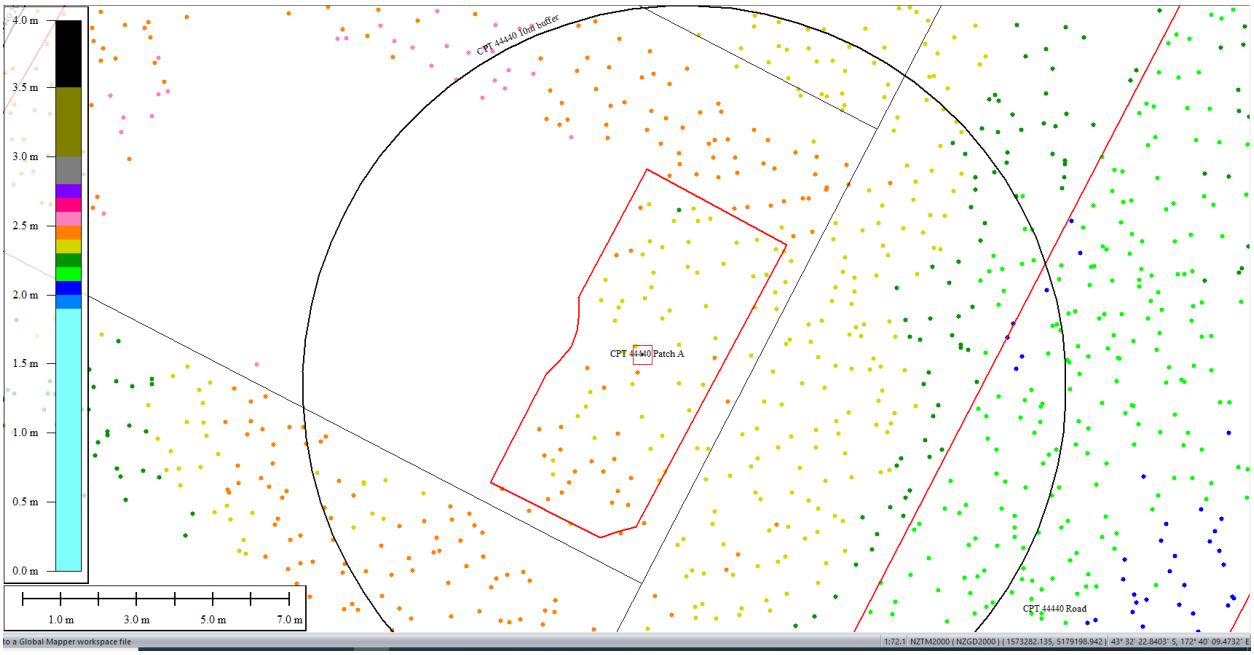

Figure 66: Ground surface elevation averaged over 10-m, 20-m, and 50-m buffers for Patch A for Sep 2011 LiDAR survey.

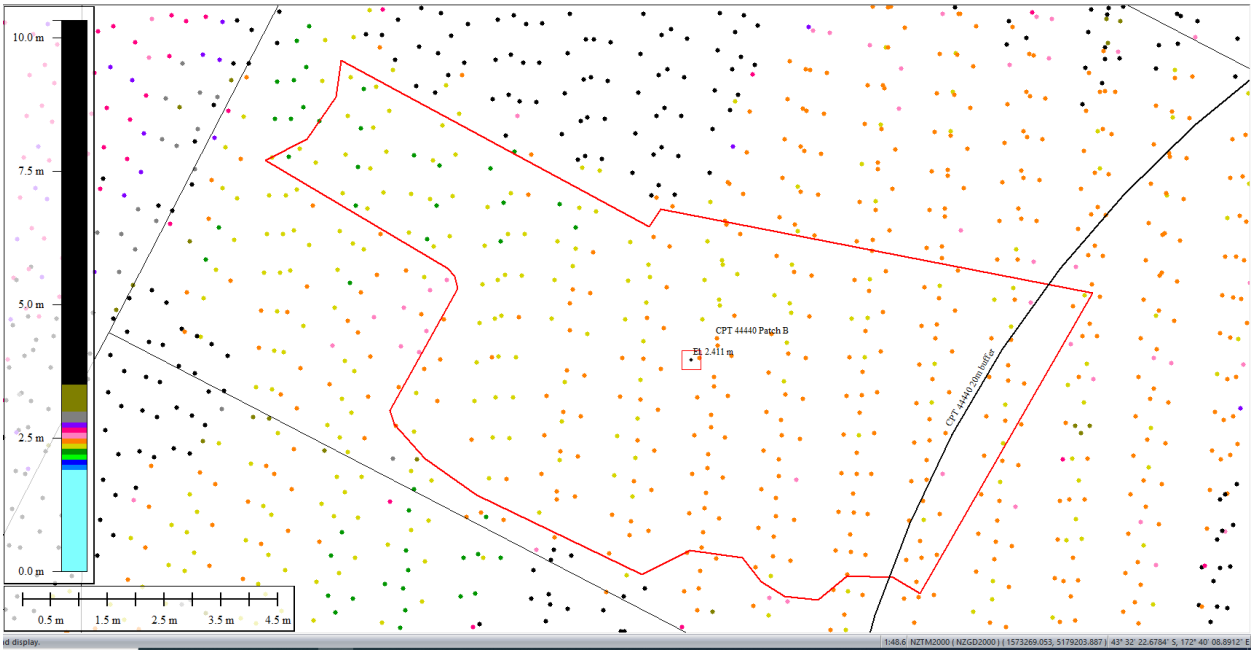

Figure 67: Ground surface elevation averaged over 50-m buffer for Patch B for Sep 2011 LiDAR survey.

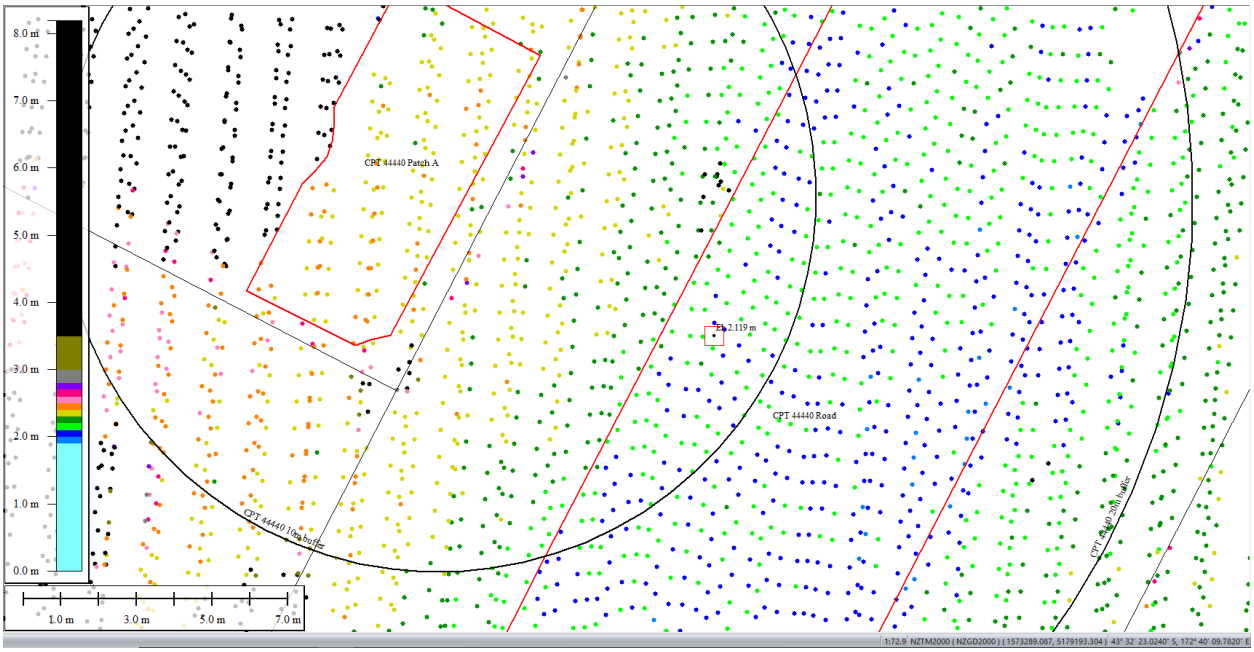

Figure 68: Ground surface elevation averaged over 10-m buffer for Road for Sep 2011 LiDAR survey.

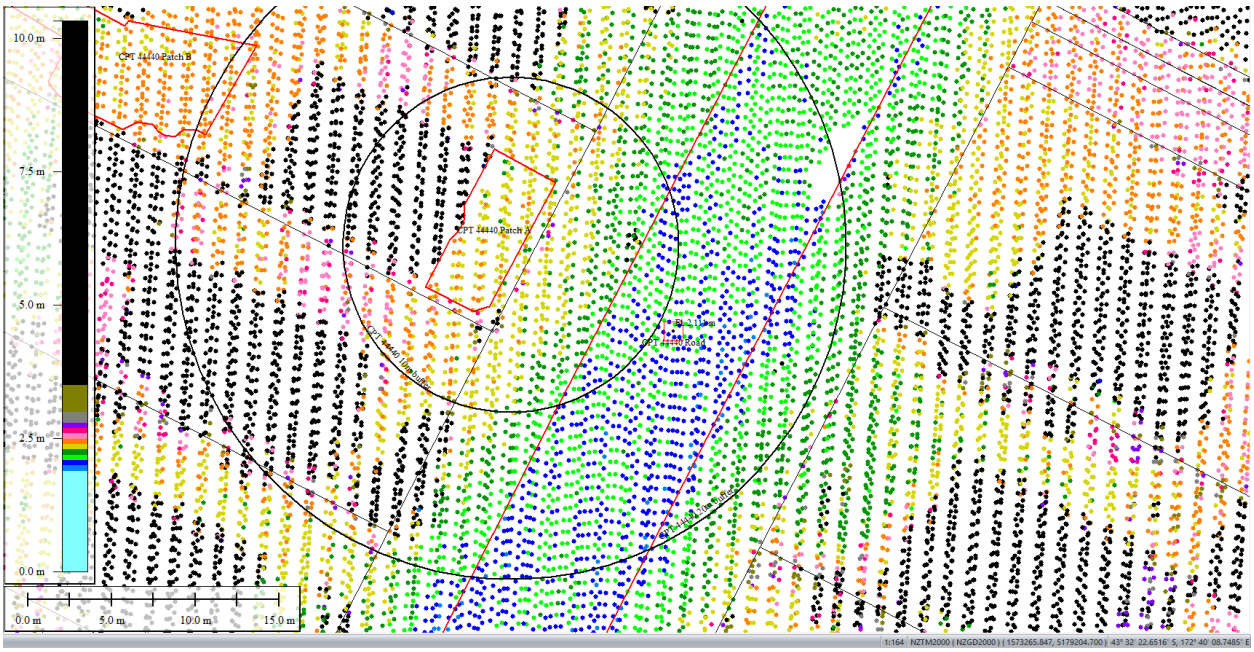

Figure 69: Ground surface elevation averaged over 20-m buffer for Road for Sep 2011 LiDAR survey.

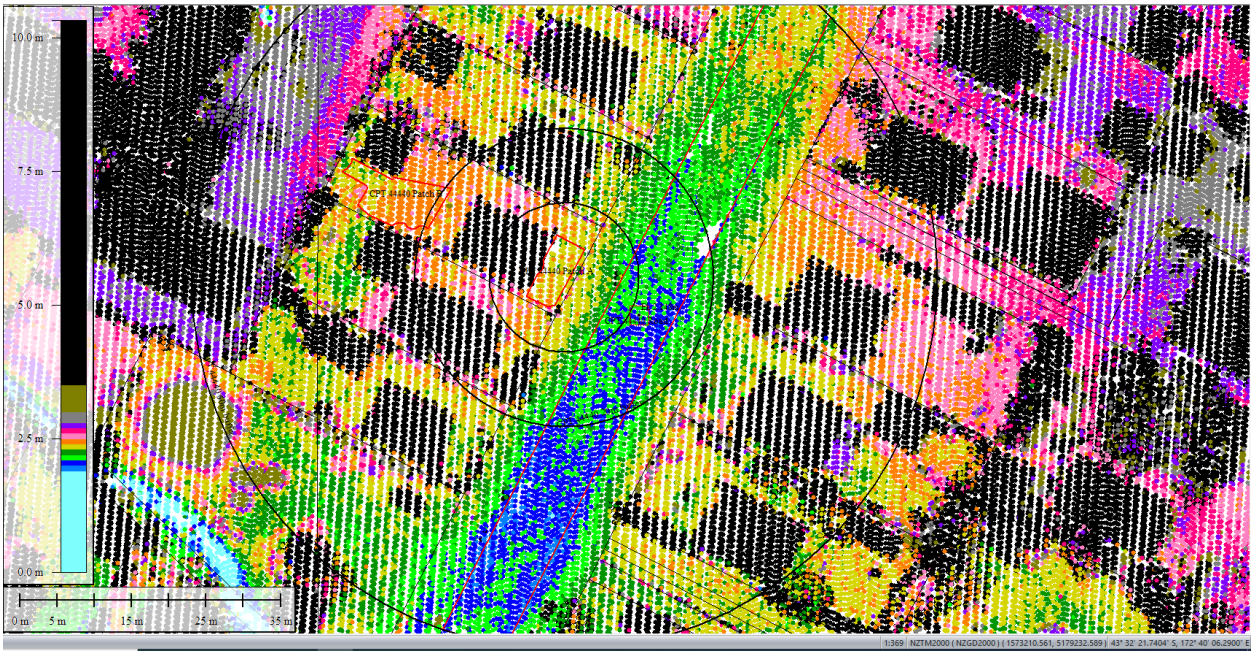

Figure 70: Ground surface elevation averaged over 50-m buffer for Road for Sep 2011 LiDAR survey.

Figure 71: Aerial photograph showing the ejecta outline at the site for Feb-11 EQ.

Figure 72: Aerial photograph acquired on 16 Jun 2011 showing the ejecta outline at the site for Jun-11 EQ.

Contents of this figure cannot be shared as doing so is restricted by a Non-Disclosure Agreement.

Figure 73: LDAT property inspection notes for Patches A and B for the Feb-11 EQ (report date: Apr 2011).

Figure 74: Ground photographs showing ejecta remnants at the property with Patches A and B (photograph date: Apr 2011).

Figure 75: Ground photographs showing ejecta remnants at properties within the 50-m buffer (photograph date: Apr 2011).

Figure 76: PGA for Sep-10 EQ (st. dev. = 0.325-0.350 ln units).

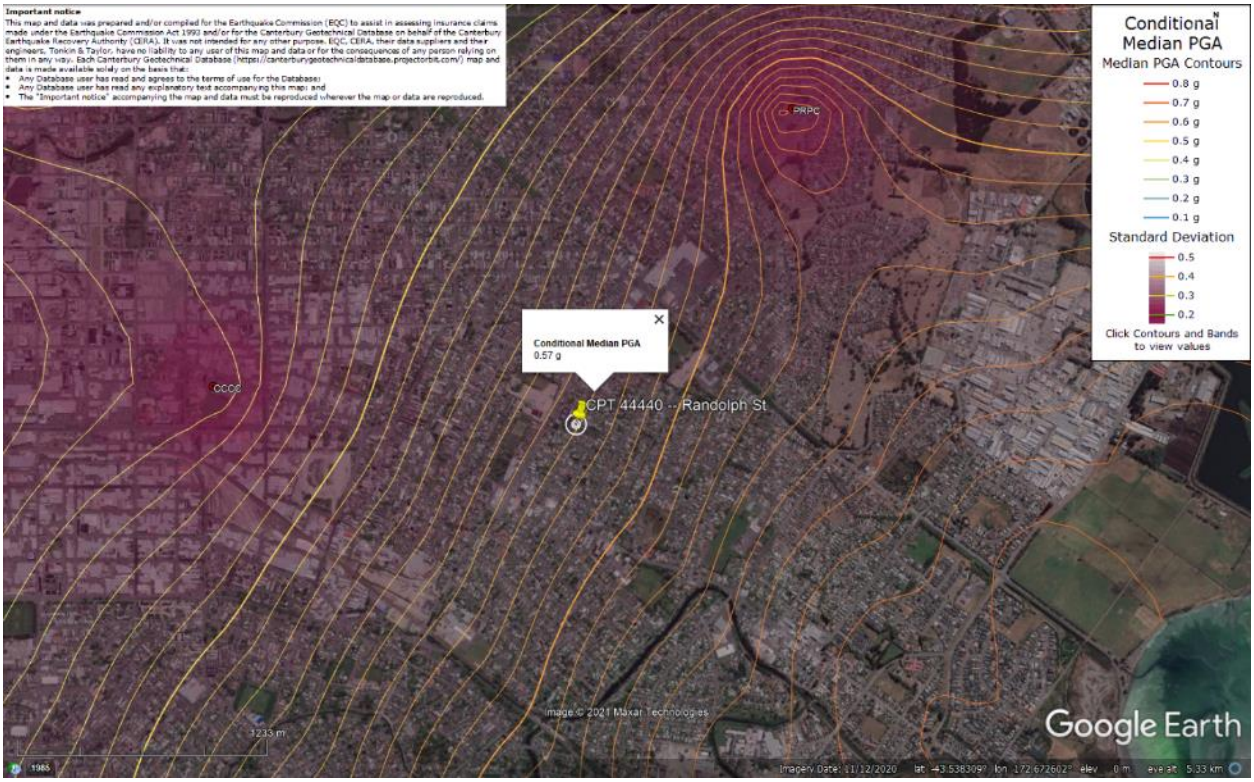

Figure 77: PGA for Feb-11 EQ (st. dev. = 0.350-0.375 ln units).

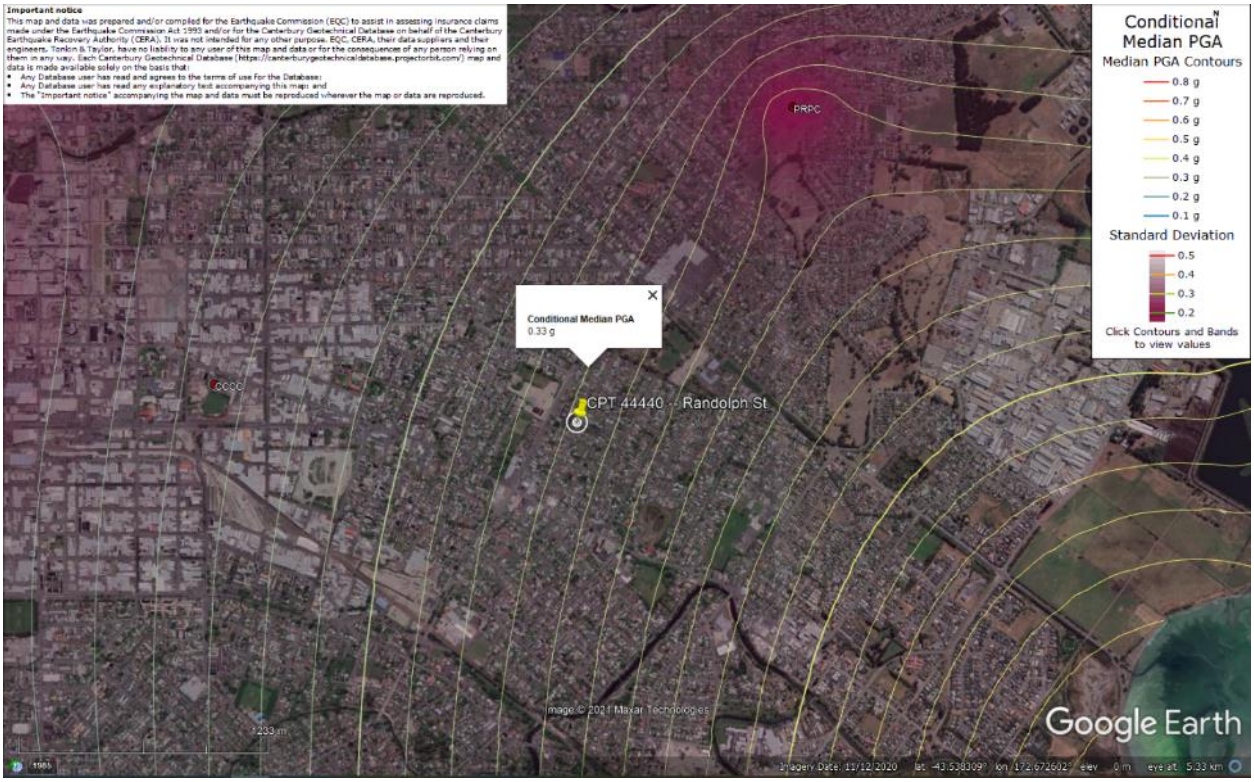

Figure 78: PGA for Jun-11 EQ (st. dev. = 0.375-0.400 ln units).

Figure 79: PGA for Dec-11 EQ (st. dev. = 0.375-0.400 ln units).

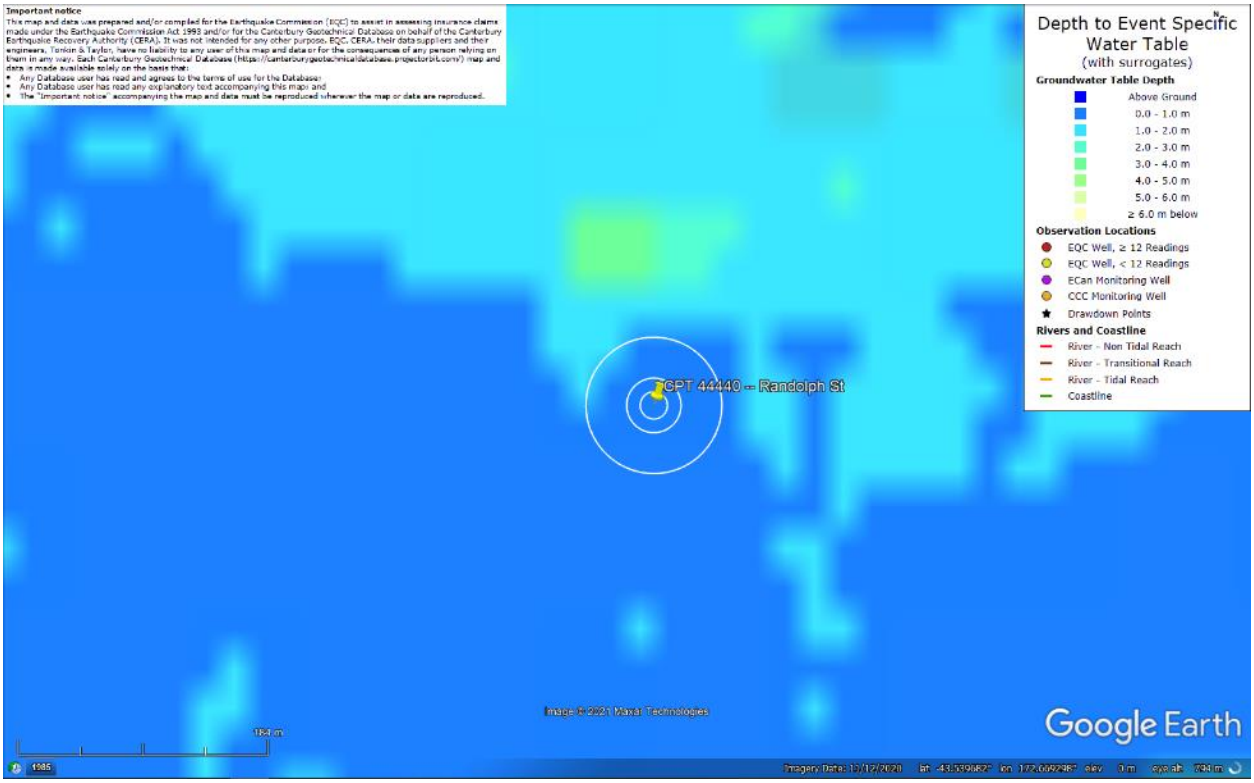

Figure 80: Depth to groundwater table for Sep-10 EQ.

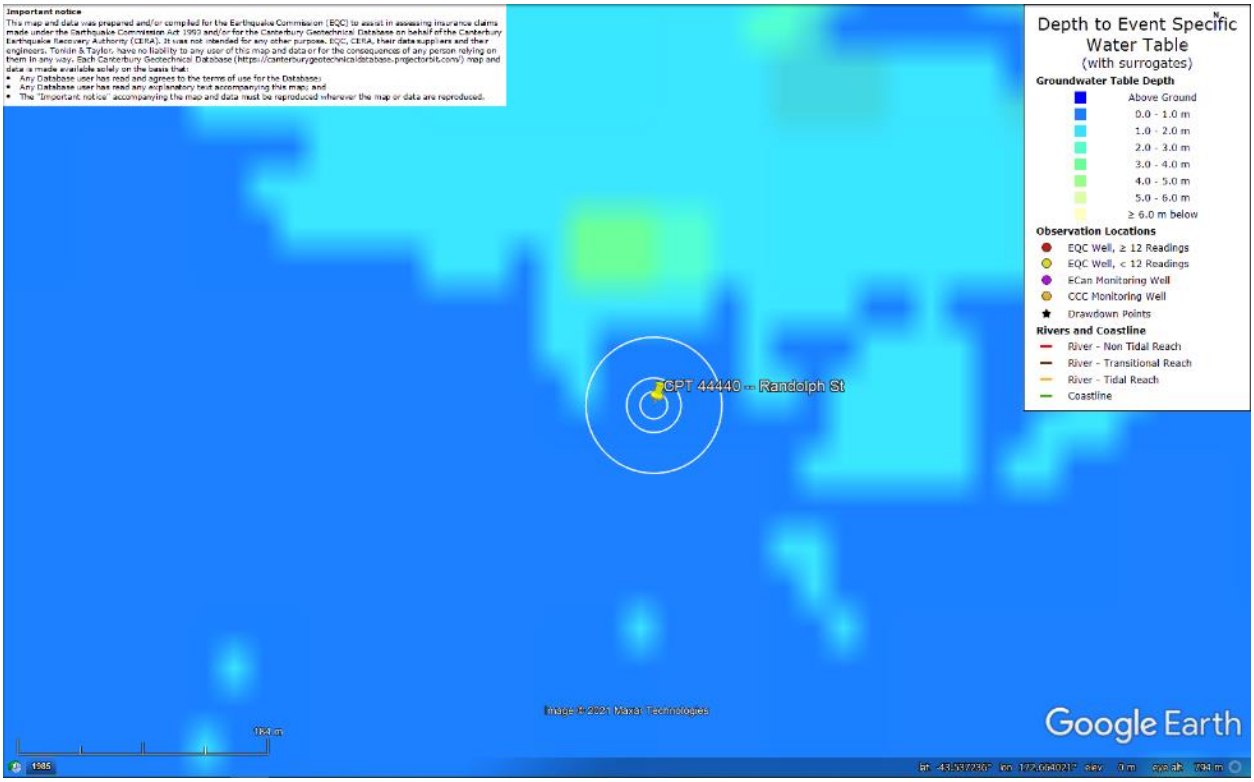

Figure 81: Depth to groundwater table for Feb-11 EQ.

Figure 82: Depth to groundwater table for Jun-11 EQ.

Figure 83: Depth to groundwater table for Dec-11 EQ.

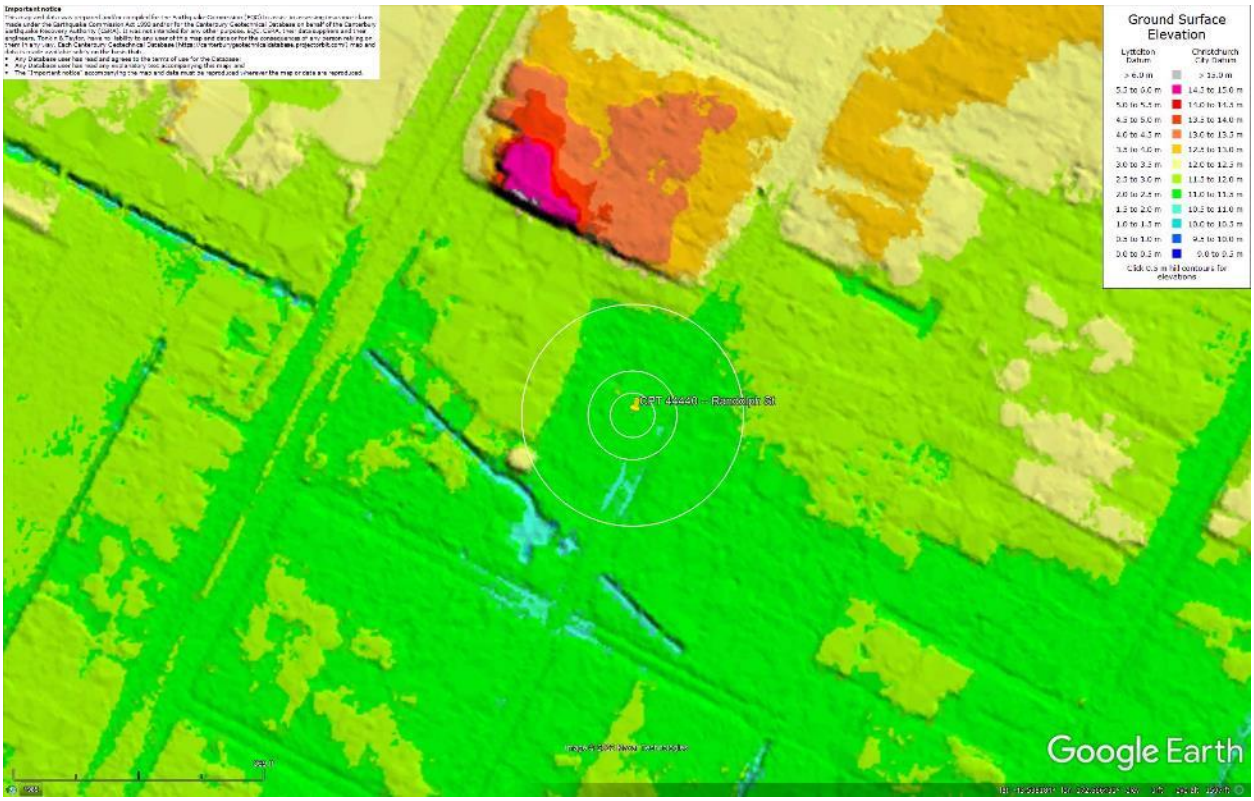

Figure 84: Ground surface elevation (Sep-11 LiDAR survey).

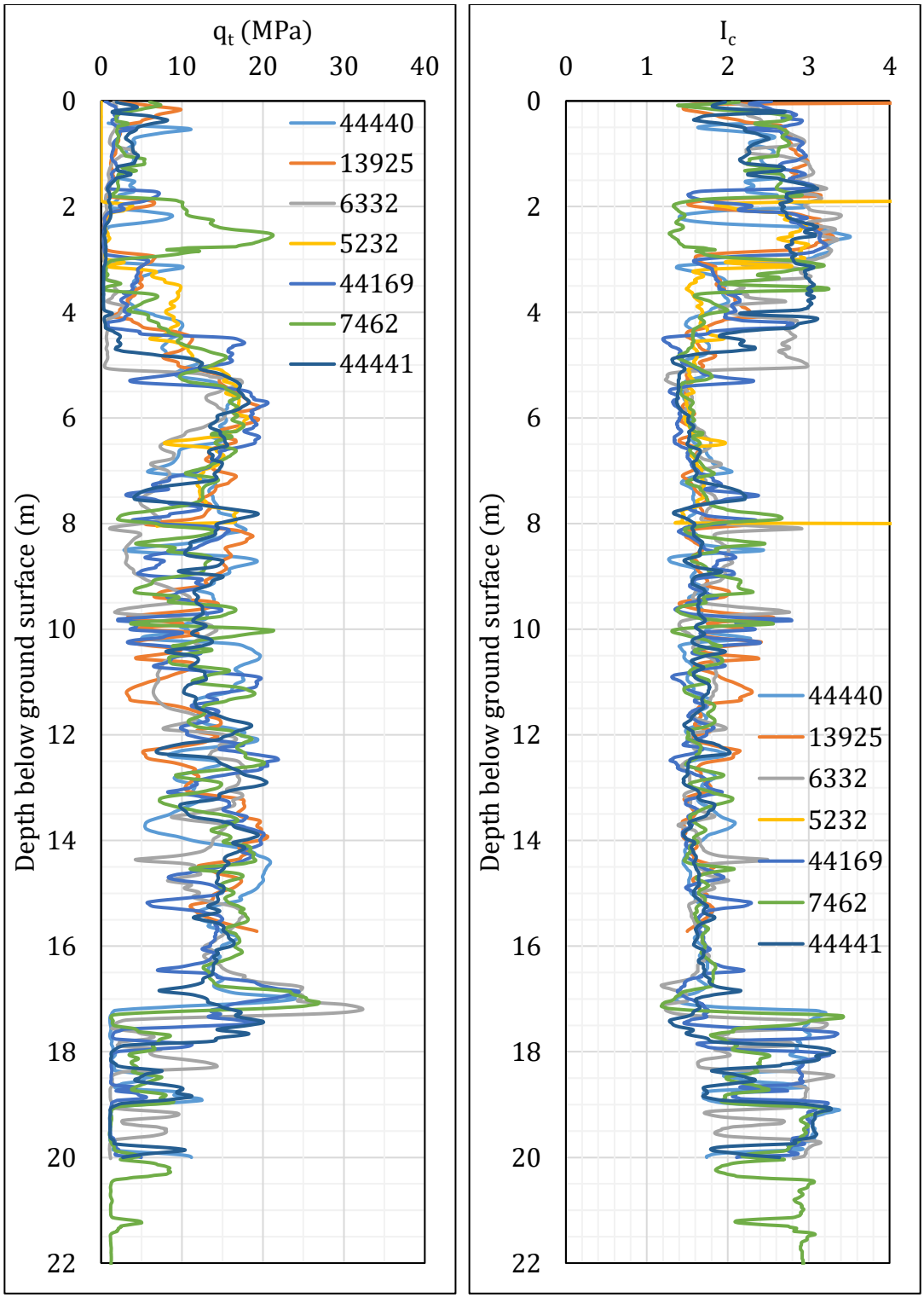

Figure 85: q_t and I_c profiles.

Note 6: The selection of CPTs for the area considered for settlement assessment (Figure 1) is based on the proximity of the CPTs to the considered areas. In accordance with that, the following table shows CPTs that were used for the volumetric settlement analysis in *Cliq v.3.0.3.2*, a CPT soil liquefaction software developed by GeoLogismiki. (The average volumetric settlements were reported in Table 8.)

Table 12: CPT profiles used in volumetric settlement analysis for areas selected for settlement assessment.

CPT ID No.	Patch A	Patch B	Road (20-m buffer)	Road (50-m buffer)
44440	✓		✓	✓
13925			✓	✓
6332		✓		
5232				✓
44169				✓
7462				
44441		✓		

Note: CPT 44440 was used to compute the volumetric settlement for a depth range from 15.72 m to 20 m, whereas CPT 6332 was used to compute the volumetric settlement for a depth range from 8.05 m to 20 m.

Table 13: CPT-based results.

		CPT ID								
EQ Event	Parameter	44440	13925	6332	5232	44169	7462	44441	$\Delta_{15.72m-20m}$	$\Delta_{8.05m-20m}$
Sep-10	S_{V1D} (mm)	109	105	191	24	140	115	100	24	127
	LSN	16	18	23	7	22	16	11	1	11
	LPI	4	7	13	2	8	5	4	0	6
	LPI_{ish}	1	4	6	1	5	1	1	--	--
	$D_{FS<1}$ (m)	3.22	1.88	3.38	3.15	1.79	3.6	4.32	--	--
Feb-11	S_{V1D} (mm)	225	184	256	57	229	229	218	44	189
	LSN	42	28	31	14	33	30	35	3	15
	LPI	28	26	32	12	30	24	21	1	18
	LPI_{ish}	26	16	19	7	22	12	19	--	--
	$D_{FS<1}$ (m)	0.72	1.84	3.38	3.15	1.67	1.82	0.56	--	--
Jun-11	S_{V1D} (mm)	151	131	213	34	177	144	138	30	148
	LSN	25	22	26	10	27	19	17	0	13
	LPI	10	12	19	4	15	10	8	0	10
	LPI_{ish}	4	7	11	2	11	5	2	--	--
	$D_{FS<1}$ (m)	3.20	1.84	3.38	3.15	1.67	3.60	4.32	--	--
Dec-11	S_{V1D} (mm)	77	84	163	19	106	91	67	17	106
	LSN	12	15	21	6	19	13	8	1	9
	LPI	3	5	11	2	6	4	3	0	5
	LPI_{ish}	0	1	5	2	2	1	1	--	--
	$D_{FS<1}$ (m)	3.22	1.90	3.38	3.15	1.81	3.60	4.32	--	--

Notes: $D_{FS<1}$ = Depth to the first liquefiable layer ($FS_L<1$) that is at least 200-mm thick, as determined by the Boulanger and Idriss (2016) liquefaction-triggering procedure (P_L=50%, C_{FC}=0.13, and $I_{c,cutoff}$ =2.6), and exported from *Cliq v.3.0.3.2*; undet. = the specified soil layer was not detected; $\Delta_{15.72m-20m}$ and $\Delta_{8.05m-20m}$ indicate S_{V1D}, LSN, and LPI values that were added to CPT 13925 and 5232, respectively, due to their shallow penetration depths.

Note 7: Based on the borehole log (BH 17183, Figure 1), the groundwater table is at a depth of 2.0 m below the ground surface. The soil profile consists of (1) silty, ML, topsoil to a depth of 0.15 m, (2) sandy silt with some fibrous organics, ML, the Yaldhurst member of the Springston formation, to a depth of 4.3 m, (3) fine to medium sand, SP, of the Christchurch formation to a depth of 17.6 m, and (4) sandy silt, ML, of the Christchurch formation to a depth of 20 m.

Note 8: The ejecta-induced free-field settlement provided in Table 11 is an areal average settlement due to ejecta, which is based on the total settlement assessment area, A_T (provided in Table 9 and repeated in Table 14). However, the considered area was not always covered completely with ejecta; thus, it is important to provide the localized ejecta-induced settlement, too. The localized settlement due to ejecta is estimated using photographic evidence only as

$$S_{E,P\_localized} = \frac{V_E}{A_E}$$

where V_E is the total volume of ejecta within A_T and A_E is the total coverage area of ejecta within A_T. Please note that the areal ejecta-induced settlement provided in Table 14 as S_{E,P_areal} is the same as $S_{E,P}$ in Table 11, which was estimated as

$$S_{E,P\_areal} = S_{E,P} = \frac{V_E}{A_T}$$

where V_E is the total volume of ejecta within A_T and A_T is the total settlement assessment area.

Table 14a: Areal and localized ejecta-induced settlement estimates for Patch A (10-, 20-, and 50-m buffers) based on photographic evidence.

Earthquake Event	A_T (m^2)	A_E (m^2)	V_E (m^3)	S_{E,P_areal} (mm)	$S_{E,P\_localized}$ (mm)
Sep-10	36.3	0	0	0	0
Feb-11	36.3	36.3	2.5-3.9	90±20	90±20
Jun-11	36.3	NA	NA	NA	NA
Dec-11	36.3	0	0	0	0

Notes: S_{E,P_areal} = $S_{E,P}$ reported in Table 11 = areal ejecta-induced settlement; $S_{E,P\_localized}$ = localized ejecta-induced settlement; A_T = total settlement assessment area; V_E = total volume of ejecta within A_T; A_E = total area of ejecta within A_T; The estimates of both areal and localized ejecta-induced settlement are rounded to the nearest 5; Final plus/minus values are also rounded to the nearest 5; NA = Not available.

Table 14b: Areal and localized ejecta-induced settlement estimates for Patch B (50-m buffer) based on photographic evidence.

Earthquake Event	A_T (m^2)	A_E (m^2)	V_E (m^3)	S_{E,P_areal} (mm)	$S_{E,P\_localized}$ (mm)
Sep-10	67.8	0	0	0	0
Feb-11	67.8	40.5	3.2-4.9	60±10	100±20
Jun-11	38.9	22.5	0.9-1.4	30±5	50±10
Dec-11	67.8	0	0	0	0

Notes: S_{E,P_areal} = $S_{E,P}$ reported in Table 11 = areal ejecta-induced settlement; $S_{E,P\_localized}$ = localized ejecta-induced settlement; A_T = total settlement assessment area; V_E = total volume of ejecta within A_T; A_E = total area of ejecta within A_T; The estimates of both areal and localized ejecta-induced settlement are rounded to the nearest 5; Final plus/minus values are also rounded to the nearest 5.

Table 14c: Areal and localized ejecta-induced settlement estimates for Road (20-m buffer) based on photographic evidence.

Earthquake Event	A_T (m^2)	A_E (m^2)	V_E (m^3)	S_{E,P_areal} (mm)	$S_{E,P\_localized}$ (mm)
Sep-10	284	0	0	0	0
Feb-11	284	284	11.4-16.7	50±10	50±10
Jun-11	249	249	2.8-5.4	15±5	15±5
Dec-11	284	0	0	0	0

Notes: S_{E,P_areal} = $S_{E,P}$ reported in Table 11 = areal ejecta-induced settlement; $S_{E,P\_localized}$ = localized ejecta-induced settlement; A_T = total settlement assessment area; V_E = total volume of ejecta within A_T; A_E = total area of ejecta within A_T; The estimates of both areal and localized ejecta-induced settlement are rounded to the nearest 5; Final plus/minus values are also rounded to the nearest 5.

Table 14d: Areal and localized ejecta-induced settlement estimates for Road (50-m buffer) based on photographic evidence.

Earthquake Event	A_T (m^2)	A_E (m^2)	V_E (m^3)	S_{E,P_areal} (mm)	$S_{E,P\_localized}$ (mm)
Sep-10	851	0	0	0	0
Feb-11	851	851	26.8-40.5	40±10	40±10
Jun-11	797	797	5.7-11.3	10±5	10±5
Dec-11	851	0	0	0	0

Notes: S_{E,P_areal} = $S_{E,P}$ reported in Table 11 = areal ejecta-induced settlement; $S_{E,P\_localized}$ = localized ejecta-induced settlement; A_T = total settlement assessment area; V_E = total volume of ejecta within A_T; A_E = total area of ejecta within A_T; The estimates of both areal and localized ejecta-induced settlement are rounded to the nearest 5; Final plus/minus values are also rounded to the nearest 5.

Summary 2:

- **The best estimate of the localized ejecta-induced free-field ground settlement at the Randolph St site for the SEP 2010, FEB 2011, JUN 2011, and DEC 2011 earthquake is 0 mm, 90±20 mm, 50±10 mm, and 0 mm, respectively.**

- **The best estimate of the localized ejecta-induced settlement of the road at the Randolph St site for the SEP 2010, FEB 2011, JUN 2011, and DEC 2011 earthquake is 0 mm, 50±10 mm, 15±5 mm, and 0 mm, respectively.**